Library

CANADA

DEPARTMENT OF ENERGY, MINES AND RESOURCES OTTAWA

A Co-operative Mines Branch and Geological Survey of Canada Research Project

TECTONIC INTERPRETATION OF ELASTIC-STRAIN-RECOVERY MEASUREMENTS AT ELLIOT LAKE, ONTARIO

H. U. BIELENSTEIN, MINING RESEARCH CENTRE

AND

G. H. EISBACHER, GEOLOGICAL SURVEY OF CANADA

October 1969

Mines Branch Research Report R 210 Price $1.00

Available by mail from the Queen's Printer, Ottawa
and at the following Canadian Government bookshops

HALIFAX
1735 Barrington Street

MONTREAL
Æterna-Vie Building, 1182 St. Catherine St. West

OTTAWA
Daly Building, Corner Mackenzie and Rideau

TORONTO
221 Yonge Street

WINNIPEG
Mall Center Bldg., 499 Portage Avenue

VANCOUVER
657 Granville Street

or through your bookseller

Price $1.00 Catalogue No. M38-1/210

Price subject to change without notice

Queen's Printer for Canada
Ottawa, 1970

Mines Branch Research Report R210

TECTONIC INTERPRETATION OF ELASTIC-STRAIN-RECOVERY MEASUREMENTS AT ELLIOT LAKE, ONTARIO

by

H.U. Bielenstein* and G.H. Eisbacher**

ABSTRACT

Bedding-plane slip, contraction faults, slickensided fractures, matrix-clast displacements, quartz veins, joints, and regional folds and faults were analysed in detail near Elliot Lake, Ontario, to test the potential of this approach for predicting the orientation of in-situ stresses in rock masses.

The major principal compressive stresses during deformation of the region were oriented subhorizontally and south-southeasterly. Gradual stress release by slow regional arching during the last 1000 million years is expressed in post-tectonic quartz veins and joints which have predominantly easterly trends.

---

* Geologist, Elliot Lake Laboratory, Mining Research Centre, Mines Branch, Department of Energy, Mines and Resources, Elliot Lake, Ontario.

** Geologist, Geological Survey of Canada, attached to the Elliot Lake Laboratory, Mining Research Centre, Mines Branch, Department of Energy, Mines and Resources, Elliot Lake, Ontario.

Measurements of in-situ state-of-stress by overcoring in vertical upholes indicate a boundary between stresses due to mining and field stresses unaffected by mining: about 3 to 6 metres above the mine roof, maximum elastic strain recovery changes from a north-south to an east-west direction.

In-situ elastic strain recovery within the field stress environment is greatest parallel to the trend of late quartz veins and joint sets. Field stresses, therefore, are interpreted as remnants of former regional tectonic stresses.

Direction des mines

Rapport de recherches R210

INTERPRÉTATION TECTONIQUE DE MESURES DE DÉTENTE D'EFFORTS ÉLASTIQUES À ELLIOT LAKE, ONTARIO

par

H.U. Bielenstein* et G.H. Eisbacher**

RÉSUMÉ

Le glissement dans le plan des couches, les failles de contraction, les fractures à miroirs de faille, les dislocations de la gangue et des sédiments, les filons de quartz, les diaclases et les plis et failles régionaux ont été analysés en détail aux environs d'Elliot Lake (Ontario) afin d'évaluer les possibilités d'une telle étude pour prévoir l'orientation des contraintes locales dans la masse rocheuse.

Les principales forces de compression qui se sont exercées lors de la déformation de la région étaient orientées en direction sud-sud-est suivant un léger pendage. La détente graduelle qui s'est traduite par un lent ploiement régional au

* Géologue, Laboratoire d'Elliot Lake, Centre de recherche minière, Direction des mines, ministère de l'Énergie, des Mines et des Ressources, Elliot Lake (Ontario).

** Géologue, Commission géologique du Canada, détaché au Laboratoire d'Elliot Lake, Centre de recherche minière, Direction des mines, ministère de l'Énergie, des Mines et des Ressources, Elliot Lake (Ontario).

cours du dernier milliard d'années est visible dans les filons de quartz et les diaclases post-tectoniques qui sont orientés principalement vers l'est.

Les mesures des contraintes locales effectuées par carottage vertical indiquent une ligne de démarcation entre les tensions dues à l'extraction minière et les tensions régionales qui n'ont pas été influencées par l'exploitation des mines: à environ 3 à 6 mètres au-dessus du toit de la mine, la détente maximale des efforts élastiques passe de l'orientation nord-sud à l'orientation est-ouest.

La détente locale des efforts élastiques dans l'ensemble des efforts régionaux est la plus prononcée en direction des filons de quartz et des groupes de diaclases récents. Par conséquent, on considère les contraintes régionales comme des vestiges d'anciens efforts tectoniques régionaux.

CONTENTS

	Page
Abstract	i
Résumé	iii
Introduction	1
PART I Regional Tectonic Analysis	2
1. Geologic Framework	4
2. Tectonic Evolution	6
3. Kinematic Analysis	9
A) Bedding-Plane Striations	10
B) Contraction Faults	12
C) Steeply Dipping, Striated Fractures	12
D) Slaty Cleavage	12
E) Flexural-Flow Folds	13
F) Matrix-Boulder Displacements	14
G) Striated Fractures in Granitic Rocks	16
H) Fracturing and Displacement of Diabase Dykes and Sills	17
I) Thrust Faults and Strike-Slip Faults	17
4. Dynamic Interpretation	20
A) Contraction Faults	21
B) Boulder-Matrix Displacements	23
C) Slip Linears in Granite	25
5. Quartz Veins, Joints and Regional Stress Relief	29
PART II Tectonic Analysis of the Rio Algom Nordic Mine	37
1. Kinematic Analysis	38
A) Bedding-Plane Slip	38
B) Contraction Faults	39
C) Steeply Dipping, Striated Fractures	39
D) Deformation of Diabase Dykes and Sills	40
2. Dynamic Interpretation	41
3. Jointing	42
PART III Reassessment of Elastic-Strain-Recovery Measurements made at Nordic Mine	43
Measurements of Elastic Strain Recovery at Nordic Mine	43
Interpretation of Field Stresses	49
Acknowledgements	54
References	55-58
APPENDIX A Schmidt Equal-Area Net	59
Planar and Linear Tectonic Fabric Elements	59
Slip Linears	59
Compression Axes	61

MAPS

Kinematic Map of Elliot Lake Region ....(in pocket)

Dynamic Map of Elliot Lake Region ....(in pocket)

Tectonic Map of Rio Algom Nordic Mine (Figure 14) ..(in pocket)

TABLE

No. Page

1. Table of Formations 5

FIGURES

1. Area covered by the regional tectonic analysis 3
2. Northerly trending cleavage re-deformed by an easterly trending fold 8
3. Striations on boulder from Gowganda Formation 15
4. Detached lens of diabase surrounded by flexural-flow folds in Bruce limestone 18
5. Conjugate contraction faults 22
6. Construction of stress axes from conjugate contraction faults on Schmidt equal-area net 22
7. Compression axes for the main deformation of the Elliot Lake region 24
8. Derivation of stress axes in two idealised cases of boulder-matrix slip 26

FIGURES (Concluded)

No.		Page
9.	Derivation of compression axes from **slip linears** on fractures in granite with varying angular relationship between compression axes and slip linears	28
10.	Late quartz veins and joints associated with small offset of bedding in Matinenda Formation	31
11.	Group of smooth joints in Mississagi Formation	31
12.	Strike frequency diagrams of joints: a)Elliot Lake region, b) Rio Algom Nordic Mine, c) Manitoulin Island	33
13.	Late post-tectonic quartz veins and joint patterns, Elliot Lake region	34
14.	Tectonic map of Rio Algom Nordic Mine ....(in pocket)	
15.	Orientation and magnitude of maximum elastic strain recovery in vertical holes	46
16.	Orientation and magnitude of maximum elastic strain recovery in horizontal holes	48
17.	Magnitude and location of maximum elastic strain recovery in horizontal and vertical holes	50
18.	Schmidt equal-area projection of planes and lines ...	60
19.	Schmidt equal-area projection of striations in a plane	62
20.	Schmidt equal-area projection of striations in a plane	63
21.	Construction of compression axes from slip linears on Schmidt equal-area net	64

==

INTRODUCTION

Determination of in-situ rock stresses by measuring elastic strain-relief in boreholes is increasingly applied in rock engineering projects. Excellent reviews of measurement techniques are available, and the reader is referred to these state-of-the-art reports for detailed information (Leeman, 1964-1965; Obert, 1966: Fairhurst, 1968; Barron, 1968).

Even before a large number of measurements had been accumulated by this technique, unexpectedly high stress values were found as a rule rather than as an exception and led several authors to suggest the possibility that tectonic stress components might be contributing factors (Hast, 1958; Obert, 1962; Coates and Grant, 1966; Hooker and Johnson, 1967; Preston, 1968).

In order to study the possible effect of tectonic controls on the state of stress around mine openings, a joint project was initiated by the Mines Branch and the Geological Survey of Canada. It comprised a detailed tectonic analysis of the Elliot Lake region (by G.H. Eisbacher), a tectonic analysis of the Nordic Mine* (by H.U. Bielenstein), and a reassessment (by H.U. Bielenstein and G.H. Eisbacher) of elastic-strain-recovery measurements made there previously by Mines Branch staff.

---

* Rio Algom Mines Limited, Nordic Division, Elliot Lake, Ontario.

PART I

REGIONAL TECTONIC ANALYSIS

In the tectonic study of small areas such as mines, tunnels, etc., a knowledge of the regional tectonic framework is essential to determine whether the small area is representative of the surrounding area, or whether it constitutes a local perturbation within a regionally uniform structural setting.

The answer to this question is critical when technical measurements, made within a small area, are to be extrapolated into the surrounding rock mass.

The tectonic analysis of the Elliot Lake region was carried out over an area shown in Figure 1. The results will be discussed under five headings: 1) Geologic Framework, 2) Tectonic Evolution, 3) Kinematic Analysis, 4) Dynamic Interpretation, and 5) Quartz Veins, Joints and Regional Stress Relief.

The two maps accompanying this regional analysis (Kinematic Map and Dynamic Map of the Elliot Lake Region) contain much of the pertinent information. In presenting data such as the orientation of slip linears (Hoeppener, 1955) and of compression axes, the equal-area projection from the lower hemisphere (Schmidt Net) is used throughout the study*.

---

* Technique explained in Appendix A.

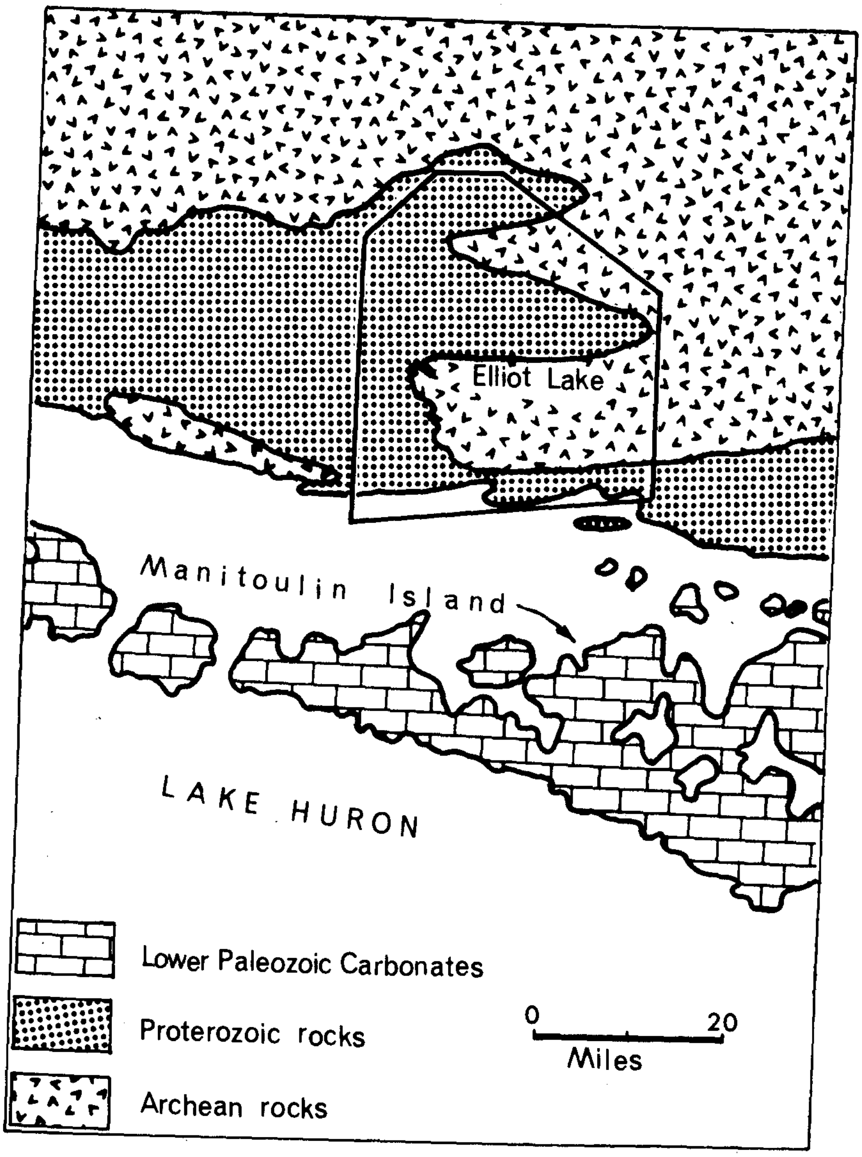

FIGURE 1: Area covered by the regional tectonic analysis.

1) Geologic Framework

Since the discovery of uraniferous conglomerate near Elliot Lake in the early nineteen-fifties, the regional geology of the Elliot Lake region has become economically important. The report and maps by Collins (1925) which guided the first staking rush have since been supplemented by work of the Geological Survey of Canada (Roscoe, 1957) and the Ontario Department of Mines (Robertson, 1961-1968). Terminology for rock units in the region has recently been reviewed (Robertson et al., 1969); the new nomenclature is being used throughout this report and is summarized in Table 1.

In the Elliot Lake region a sequence of Proterozoic ("Huronian") sedimentary rocks up to 7000 feet thick rests unconformably on Archean granite and greenstone-greywacke complexes. The age of the Archean granites was radiometrically determined as 2500 m.y.* (Van Schmus, 1965).

The deposition of the Huronian sedimentary sequence began with the accumulation of quartz-pebble conglomerate in northwesterly trending channels, which were cut into less resistant greenstones rather than into massive granite (Pienaar, 1963; Roscoe, 1957). These quartz-pebble conglomerates contain the uranium ore that is mined in the Elliot Lake region. Quartz-pebble conglomerate and interlayered coarse-grained feldspathic

---

* million years.

TABLE 1

Table of Formations

Nipissing Diabase

Intrusive Contact

COBALT GROUP	Bar River Formation	
	Gordon Lake Formation	
	Lorrain Formation	
	Gowganda Formation	
QUIRKE LAKE GROUP	Serpent Formation	
	Espanola Formation	Espanola greywacke
		Bruce limestone
	Bruce Formation	
HOUGH LAKE GROUP	Mississagi Formation	
	Pecors Formation	
	Ramsay Lake Formation	
ELLIOT LAKE GROUP	McKim Formation	
	Matinenda Formation	

Unconformity

ARCHEAN

quartz sandstones and grits (often misleadingly referred to as 'quartzites') constitute the rock type which is mined around Elliot Lake. Quartz-pebble conglomerate, feldspathic quartz sandstones and grits comprise the Matinenda Formation. The Matinenda Formation is overlain by a sedimentary succession, which consists of a threefold repetition of conglomerate, argillite (or minor limestone), and quartz sandstone (Roscoe, 1957; Pienaar, 1963). The sedimentary section and the underlying granite-greenstone basement were intruded by diabase ('Nipissing' Diabase) about 2100 m.y. ago (Van Schmus, 1965), and by granite ('Cutler' Granite) about 1750 m.y. ago (Van Schmus, 1965).

2) Tectonic Evolution

To understand the kinematics and dynamics of structural features in the region, chronological succession and areal extent of tectonic events had to be analysed.

Five steps can be clearly identified in the tectonic evolution:

A) Early faulting along northerly and easterly trending basement fractures occurred during and shortly after deposition of the sedimentary rocks. Displacements along these fractures appeared as contemporaneous normal faults in partly consolidated rocks of the Espanola Formation (Eisbacher, in press).

B) Faults trending N10°E-N20°E continued to move after deposition of the sedimentary pile and led to easterly directed upthrusts within sedimentary units. Close to these faults (Batty Lake Fault, Hough Lake Fault, Gullbeak Lake Fault) and parallel to them, slaty cleavage was formed in argillaceous units.

C) 2100 m.y. ago Nipissing Diabase intruded the Huronian sedimentary rocks and basement complex. The alignment of the large diabase bodies along northerly and easterly trends suggests that intrusion followed pre-existing basement fractures.

D) After the intrusion of Nipissing Diabase and Cutler Granite the whole region was deformed by local shortening and differential vertical motion of basement blocks. This relatively penetrative deformation imprinted the principal easterly trending structures and the bulk of the tectonic fabric presently seen in the Elliot Lake region. It also re-deformed earlier structures such as northerly trending cleavage (Figure 2). Deformation must have occurred after emplacement of the Cutler Granite (1750 m.y.), which was involved in this orogenic phase, and prior to 1200 m.y., which is the age of intrusion for essentially undeformed olivine diabase dykes (Van Schmus, 1965).

FIGURE 2: Northerly trending cleavage re-deformed by an easterly trending fold, looking northwest (Whiskey Lake).

E) Continuing small differential uplift and broad regional arching led to the development of thin quartz veins and joints.

The sequence of events given above differs slightly from previous models of the tectonic evolution within the Elliot Lake region (e.g. Robertson, 1962). In contrast to these models, the present authors emphasize that the intrusion of the Nipissing Diabase bodies may separate an early deformational stage, dominated by northerly trending basement faults, from a later, more penetrative deformation which produced the easterly trending structures of the Elliot Lake region. Much of the deformation within the Huronian sedimentary sequence was controlled by displacements within the Archean basement. Tectonic shortening within the Quirke Syncline was small and amounts to about 5% (see Figure 7, on page 24).

3) Kinematic Analysis

Regional kinematic analysis of deformed rocks is based on tectonic study of individual outcrops. If deformation has been sufficiently penetrative each outcrop should contain traces of displacement and strain. Orientation and, if possible, magnitude of these local traces of deformation were measured and recorded systematically.

Integrating the outcrop analyses on a regional scale makes it possible to resolve large folds, faults and fracture patterns into their components of motion. By this procedure, large-scale faults and folds can be understood in terms of displacements, rotational axes, and strain.

In the Elliot Lake region the following tectonic fabric elements were used in the kinematic analysis:

A) Bedding-plane striations (in bedded quartzose units);

B) Contraction faults (in bedded units);

C) Steeply dipping, striated fractures (in bedded units);

D) Slaty cleavage (in argillaceous units);

E) Flexural-flow folds (in limestone and argillaceous units);

F) Matrix-boulder displacements (in matrix-rich conglomerates);

G) Striated fractures in massive granitic rocks;

H) Fracturing and displacement of diabase dykes and sills;

I) Thrust faults and strike-slip faults.

A) Bedding-Plane Striations

Tectonically polished and striated (slickensided) bedding surfaces are commonly found in bedded quartzose units. They were noted and correctly interpreted by all previous workers in the region (Roscoe, 1957; Pienaar, 1963; Robertson, 1961-1968).

Although most of the quartzose, well bedded, rock masses show intense internal cataclasis (Roscoe, 1957), the ubiquitous occurrence of bedding-plane slip linears indicates that failure commonly occurred by slip along bedding surfaces.

Tectonically lineated bedding planes are covered with a thin quartz coating which displays distinct steps perpendicular to the lineation. By determining the orientation of 'congruous accretion' steps (Norris and Barron, 1969), the sense of displacement could be found.

Bedding-plane slip linears are presented on the Kinematic Map as arrows indicating the direction of motion of the hangingwall. The distribution and orientation of bedding-plane striations show that movement occurred predominantly in northerly and southerly directions. Deviations from this trend are particularly conspicuous in areas where the greenstone-greywacke complex abuts against the granitic basement. In these localities (e.g. west of Nordic Mine, and the area at the northeastern corner of the Kinematic Map), slip linears tend to align themselves perpendicular to the boundary between the granitic basement and the mechanically less competent greenstone-greywacke basement.

The nodes of divergence and convergence of slip linears define the axial surface of a syncline ('Quirke Syncline') and anticline ('Chiblow Anticline') respectively, delimiting the nature of the last stages of interbed slip in the area.

Characteristically, none of the northerly trending older structures is strongly expressed in terms of bedding-plane slip linears. A reason for this could be the incomplete consolidation of quartzose units during the early deformation.

B) Contraction Faults

Contraction faults (Norris, 1958) occur where slip parallel to bedding planes is transferred to fractures that cut across bedding (Figure 5). Contraction faults are generally inclined at about 10° to 30° to bedding (Norris, 1958; R.A. Price, 1967). Throughout the Proterozoic sequence the sense of displacement on contraction faults was found to conform with that derived from bedding-plane slip.

C) Steeply Dipping, Striated Fractures

Steeply dipping, striated fractures in quartzose sedimentary rocks have northerly and northwesterly trends. Their surfaces are coated with chlorite and other brownish weathering minerals. Striations are predominantly subhorizontal and displacement is right-lateral on northwesterly trending fractures and left-lateral on northerly trending fractures. Steeply dipping, striated fractures are generally found close to strike-slip faults.

D) Slaty Cleavage

While well-bedded quartzose units in the area failed largely by bedding-plane slip and along contraction faults, argillaceous units deformed by more penetrative flow. This flow led to preferred orientation of micaceous particles parallel to well-defined surfaces. These surfaces are now expressed as slaty cleavage in the rock mass.

Along the limbs of a fold, the kinematics of slaty cleavage are equivalent to bedding-plane slip in terms of relative displacements, with the distinction that slaty cleavage reflects a finite state of strain whereas bedding-plane slip constitutes discrete displacement between individual plates of rock.

As mentioned previously, slaty cleavage was not only formed during the second, very penetrative deformation of the area, but locally also during early movement along north-northeasterly trending faults. In a few places (e.g. east of Batty Lake Fault), this older cleavage has been rotated by folds generated during the younger, more penetrative deformation.

The trend of cleavage surfaces is plotted on the Kinematic Map. It is generally normal to and compatible with movements indicated by bedding-plane striations.

E) Flexural-flow Folds

Flexural-flow folds are commonly observed within the calcareous units of the Espanola Formation (Bruce limestone). Siliceous beds, interlayered with the incompetent limestone, were buckled into small folds with easterly trending axes during deformation of the sedimentary succession. Flowage of limestone rotated the axial surfaces of these folds into an inclined attitude. The resulting vergence of small-scale folds generally conforms to the sense of displacement shown by bedding-plane slip.

On the Kinematic Map the axes of flexural-flow folds are plotted as rotational axes.

F) Matrix-boulder Displacements

The Proterozoic section of the Elliot Lake region contains three conglomerate units which are strikingly different from the basal quartz-pebble conglomerate. They are characterized by well-rounded boulders and cobbles of granite, embedded in a matrix of chlorite, feldspar and quartz. These conglomerates make up the bulk of the Ramsay Lake Formation, Bruce Formation and Gowganda Formation.

During the main deformation, a weak cleavage was imprinted upon the matrix and slight displacements occurred between boulders and surrounding matrix. These displacements are commonly expressed by an intricate system of striations along the tectonically polished boulder-matrix boundary (Figure 3). Differential slip between boulders and matrix, in places, led to cracks within boulders and across the boulder-matrix boundary. Striations on boulders and cobbles were measured at seven localities within the Quirke Syncline: one in Ramsay Lake conglomerate and six in Gowganda conglomerate.

For each locality, slip linears and poles to fractures were plotted on the equal-area net. The resulting diagrams are

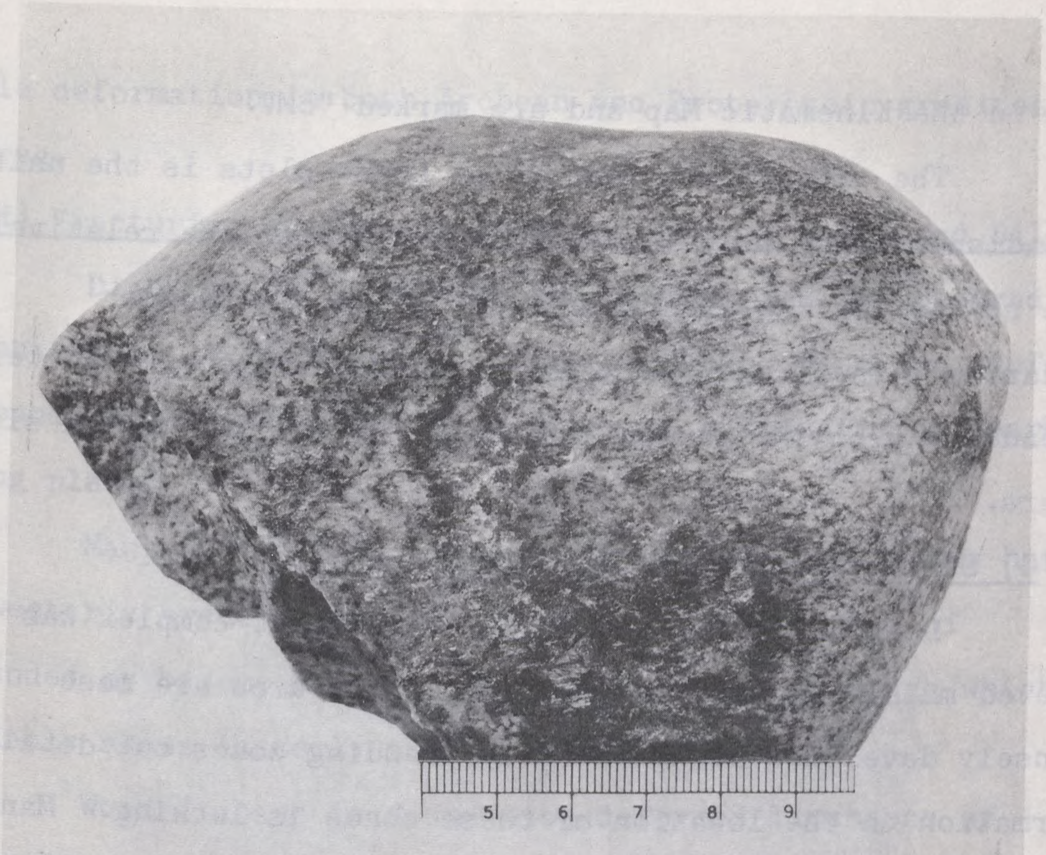

FIGURE 3: Striations on boulder from Gowganda Formation.

shown on the Kinematic Map and are marked "BM".

The significant feature in these plots is the uniform trend displayed by slip linears, regardless of the relatively large scatter in the orientation of the matrix-boulder boundaries. The fractures across the boulders strike easterly, perpendicular to the general trend of the boulder-matrix slip linears.

G) Striated Fractures in Granitic Rocks

Deformation of the granitic basement complex was achieved mainly by brittle fracture. Fractures are most intensely developed along easterly trending zones but detailed information on the location of these zones is lacking. Many of the fractures are seen to offset veins and inclusions in the granite, and striations are commonly observed on exposed fracture surfaces.

Striations with known sense of displacement were measured in the field, and plotted on equal-area diagrams (marked "G" on the Kinematic Map). Definite trends of slip linears (northerly to north-northwesterly) show up in all diagrams, regardless of scatter in the orientation of fracture surfaces. Diagrams of slip linears from the Cutler Granite show the same trend as do the slip linears from basement granite immediately north of the Murray Fault. This observation points to mechanical equivalence, and probably contemporaneity of brittle deformation, in both Archean and Proterozoic granites of the area.

H) Fracturing and Displacement of Diabase Dykes and Sills

Diabase bodies are intensely fractured and sheared at many outcrops. Striations on gently inclinded fracture surfaces are found to be of similar orientation as striations on nearby bedding planes.

Many of the thin, steeply dipping diabase dykes have northwesterly trends. Several of these, particularly if surrounded by basement rocks, display tectonic cleavage which invariably shows easterly trends.

When diabase is found with deformed limestone or argillaceous units, it is commonly seen to be sheared into individual lenses (Figure 4).

All these features, mentioned above, document the intensive deformation which took place after the intrusion of diabase.

I) Thrust Faults and Strike-Slip Faults

Within the Proterozoic sequence, major offsets of stratigraphic boundaries are related to thrust faults and strike-slip faults. Along thrust faults and strike-slip faults, rock masses are generally shattered over tens of feet, particularly in cases where heterogeneous bodies such as diabase dykes are involved. Strike-slip faults are seen to offset

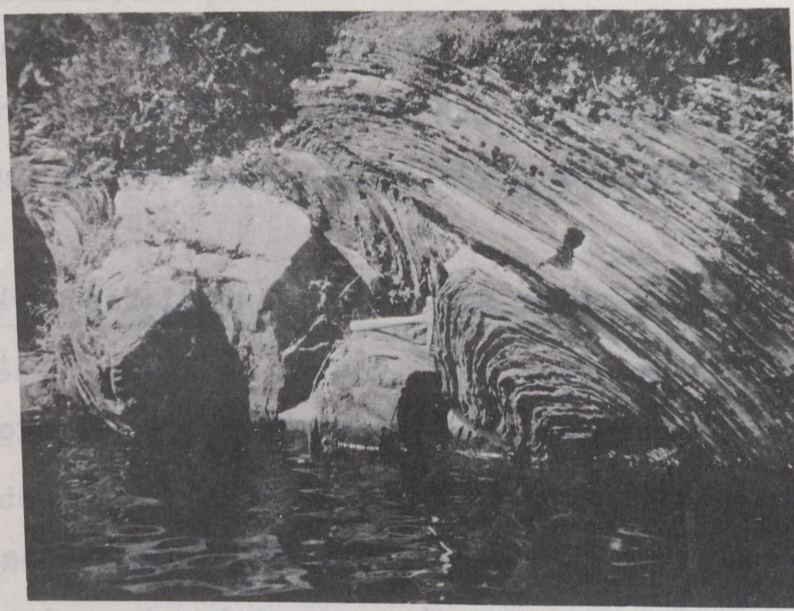

FIGURE 4: Detached lens of diabase (left of hammer) surrounded by flexural-flow folds in Bruce limestone (McCabe Lake).

thrust faults in several places (e.g. near Denison Mine and north of Elliot Lake). But, on the other hand, they also seem to control domains of different bedding-plane slip and thrusting. Therefore, no distinct break in time between thrust faulting and strike-slip faulting can be documented.

a) Thrust Faults

The three steeply dipping, north-northeasterly trending upthrusts, Gullbeak Lake Fault, Hough Lake Fault, Batty Lake Fault, formed during the first, pre-diabase, deformation of the area. Large diabase bodies along the Hough Lake Fault and the Batty Lake Fault seem to have intruded partly along the faults and obscured parts of their pre-diabase course. Both the faults and the diabases are seen to be cut and re-deformed by later, easterly trending faults.

Easterly trending thrust faults are associated with the second, more intense, deformation of the area. Within the higher parts of the Proterozoic succession, thrust faults are a combination of bedding-plane slip and contraction faulting; their dip is generally less than 40°. Close to the basement, thrust surfaces steepen considerably (e.g. Lake of the Mountains Fault). Finally, within basement rocks, faults are replaced by complicated fracture zones. For most thrusts, involvement of basement can be demonstrated (Flack Lake Fault, and several faults in the northeastern part of the Quirke Syncline). Parts of other thrusts are probably due to detachment of competent stratigraphic units from other less competent units beneath (Nordic Fault, Quirke Lake Fault).

Along the base of the sedimentary succession no marked detachment took place.

b) Strike-Slip Faults

The major strike-slip faults in the area all have northwesterly trends (Moon Lake Fault, Horne Lake Fault, Pecors Lake Fault, Spanish American Fault). Stratigraphic offsets and subhorizontal striations on nearly vertical fractures within the fault zones indicate right-lateral displacements.

Northerly trending, strike-slip faults are few in number and generally short (e.g. fault near Denison Mine). The displacement on these faults is left-lateral.

Late displacement along the Murray Fault was also strike-slip and right-lateral. In several localities along the Murray Fault, subhorizontal striations are seen to be overprinted on early, steeply pitching striations (Eisbacher, 1969).

Deformation along strike-slip faults passes without noticeable break from the sedimentary cover into basement rocks.

4) Dynamic Interpretation

If strains, recorded in rocks, are small and the rock mass can be considered isotropic before deformation, a dynamic interpretation of the strains may be feasible. In such cases detailed statistical analysis of the deformational mechanisms may permit the derivation of the orientation of compatible stress tensors.

Contraction faults, boulder-matrix displacements, and slip linears in granite were used to derive the orientation of local stress fields compatible with the deformation of the Elliot Lake region.

A) Contraction Faults

Contraction faults which start as bedding-plane slips and, after cutting across bedding, continue as bedding-plane slips, generally cannot be used to infer a unique orientation for the stress tensor.

Locally, contraction faults were seen to cut across bedding in opposite direction but at about equal angles to bedding. Such sets of conjugate contraction faults indicate that the major principal compressive stress σ_1* must have been aligned approximately parallel to bedding when the two sets of contraction faults formed (Figure 5). The intermediate axis σ_2 should have been parallel to the strike of the contraction faults, and σ_3 about perpendicular to bedding.

Statistically, stress axes can be derived by the use

* Compressive stress is taken to be positive, and principal stresses are labelled $\sigma_1 > \sigma_2 > \sigma_3$.

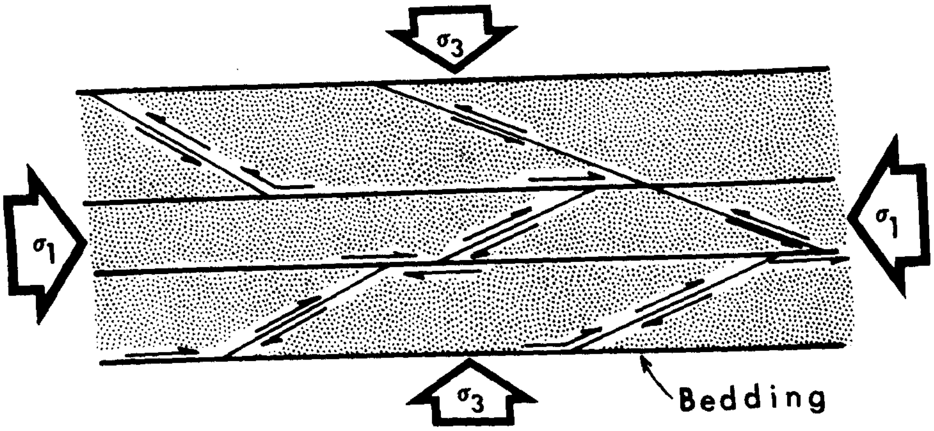

FIGURE 5: Conjugate contraction faults.

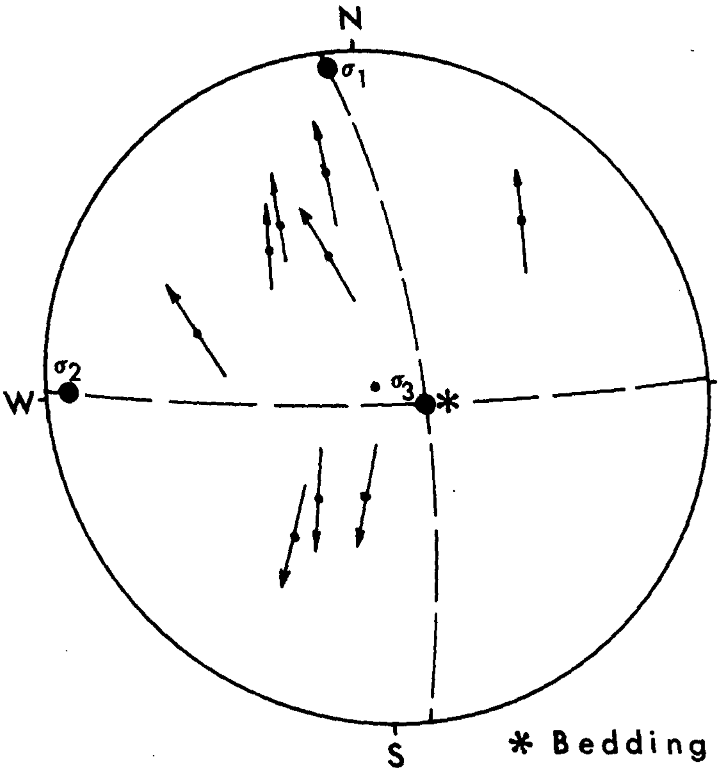

FIGURE 6: Construction of stress axes from conjugate contraction faults on Schmidt equal-area net.

of the Schmidt Net, provided a number of conjugate contraction faults are found within a certain domain. The striations measured on the contraction faults are plotted on the equal-area net (Figure 6). The great circle from which the slip linears diverge represents the principal plane, which contains σ_2 and σ_3. A surface parallel to the trend of the slip linears, plotted as a second great circle, contains σ_1 and σ_3. The intersection of these two great circles gives the orientation of σ_3; σ_1 and σ_2 can be gained by geometrical construction on the two great circles.

A sufficient number of contraction faults for this type of analysis was found at three localities in the core of the Quirke Syncline. The orientation of the major principal compressive stress axis (σ_1) is subhorizontal and oriented in a northerly direction. The axes of compression for the three localities are plotted on the Dynamic Map (marked with "C") and on Figure 7.

B) Boulder-matrix Displacements

Boulder-matrix displacements were studied in the Ramsay Lake conglomerate (one outcrop) and in conglomerate of the Gowganda Formation (six outcrops).

The kinematics of the displacements have been described in a previous section. Strains within the matrix, and displacements along the boulder-matrix boundary, are small;

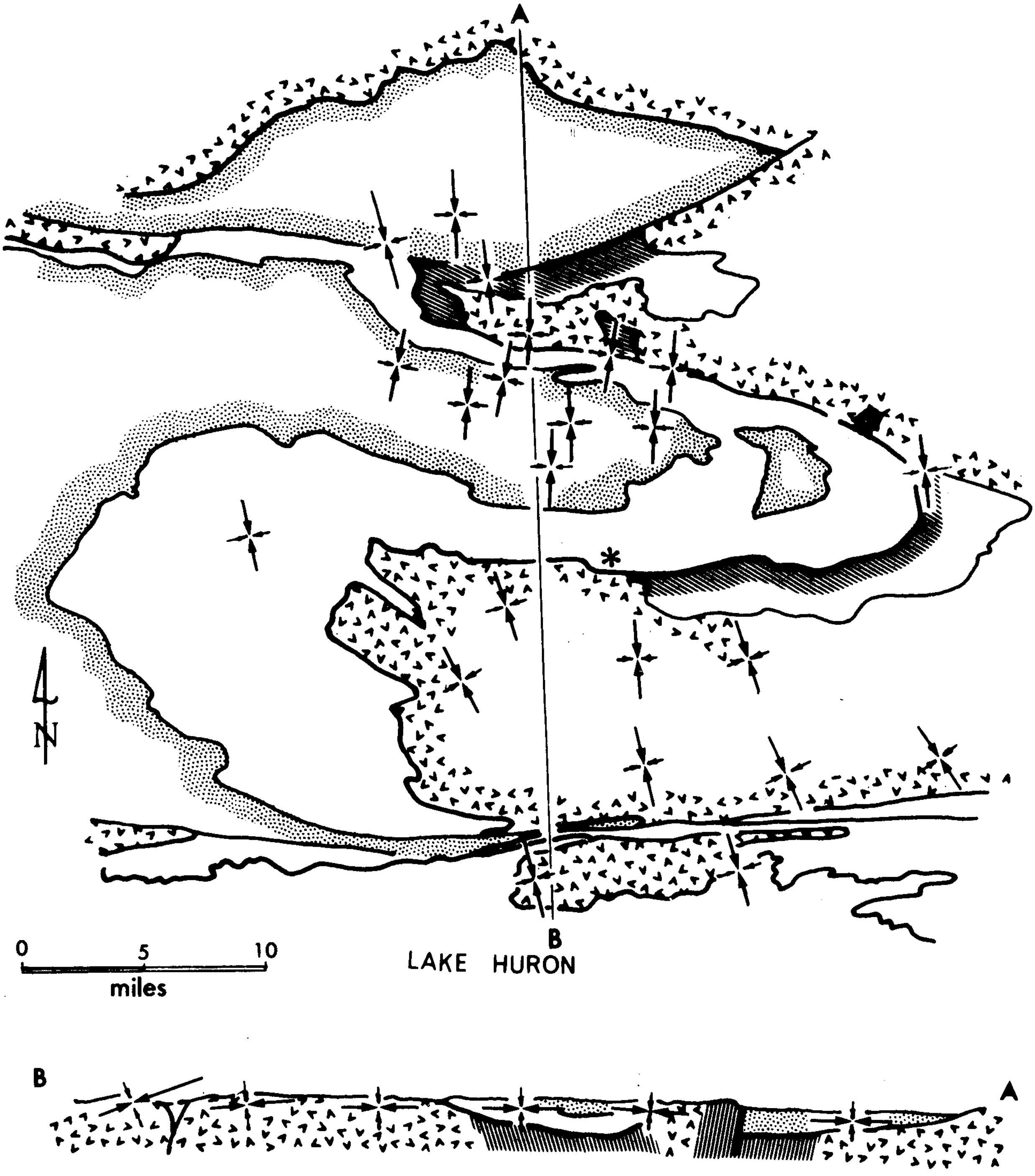

FIGURE 7: Compression axes for the main deformation of the Elliot Lake region. Long arrows represent σ_1.

therefore, a dynamic interpretation of the diagrams shown on the Kinematic Map seems to be feasible.

If slip along the boulder boundaries converged at two points on opposite sides of the boulder surface, slip linears in the diagram would radiate with respect to the pole which marks the line connecting these points (Figure 8a); this pole could be considered as parallel with the σ_3 axis, which in this case would be the only stress axis fixed in space. The σ_1 and σ_2 axes would have an indeterminate position on the great circle marking the plane perpendicular to the σ_3 axis.

In reality, slip linears trend parallel to a plane (great circle containing σ_1 and σ_3) and diverge from a plane (great circle containing σ_3 and σ_2). The intersection of these two circles renders the σ_3 axis. σ_1 and σ_2 can be found by construction (Figure 8b). The orientation of the major principal compressive axis σ_1 was found to be subhorizontal to slightly inclined to the north and north-northeast.

Axes of compression found by this technique are plotted on the Dynamic Map (marked "BM") and Figure 7.

C) Slip Linears in Granite

The granite complex which makes up the bulk of the basement in the Elliot Lake region is considered to have been mechanically isotropic previous to its brittle failure. Weakly foliated inclusions may not strictly satisfy this assumption at

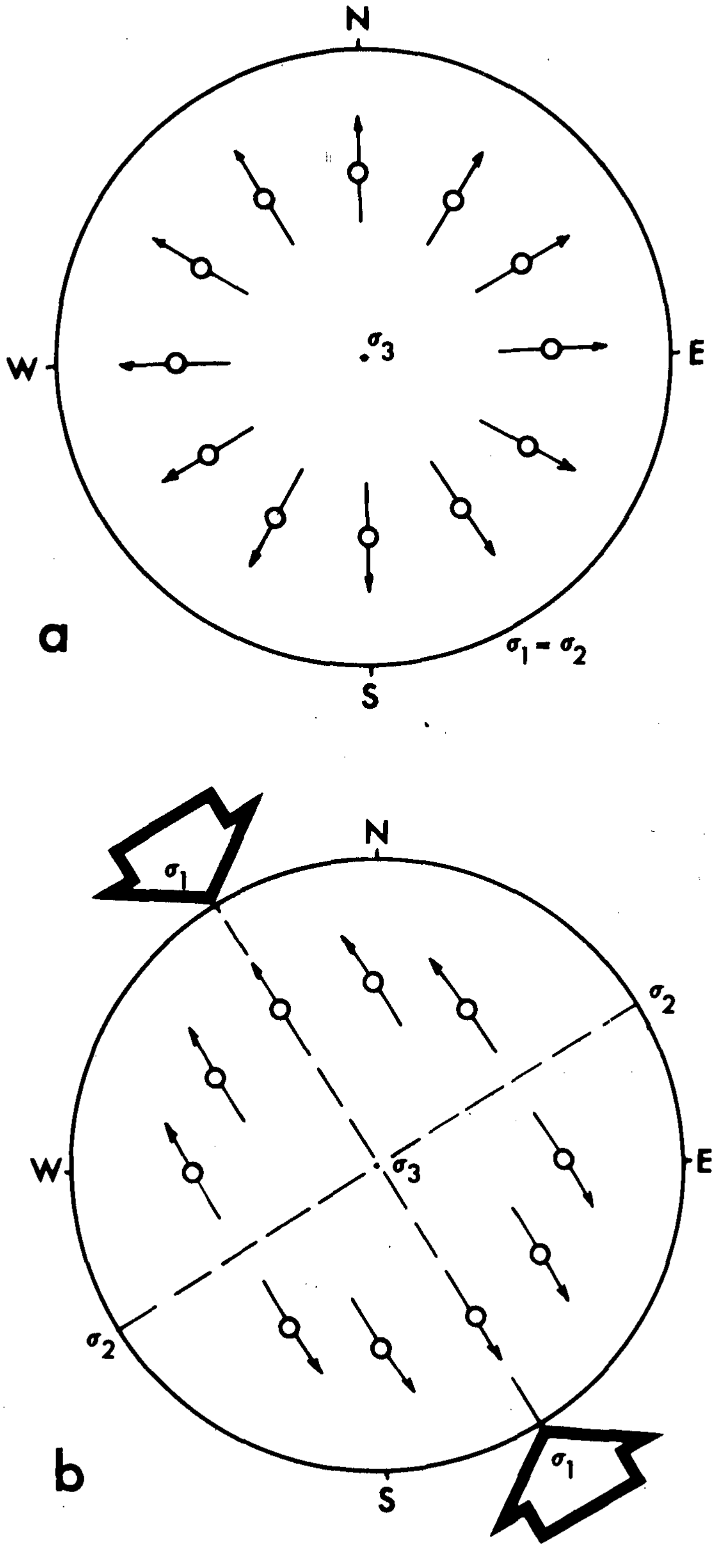

FIGURE 8: Derivation of stress axes in two idealised cases of boulder-matrix slip: a) radial slip linears, b) slip linears parallel to great circle.

a few localities.

Offsets that can be matched across fractures rarely exceed several feet. Thus, seen on a regional scale, deformation created by the individual fracture is small.

To find the orientation of a compatible stress field for the brittle deformation, a method slightly modified from one proposed by Compton (1966) was used.

Each slip linear shown in the diagrams of the Kinematic Map was related to the compressive stresses during deformation; the stress axes σ_1 and σ_3 must fall on the great circle which defines the slip linear. For several diagrams, angles of 60°, 45°, 30°, and 15° were assumed as angles of failure (angle between slip linear and major principal stress). For each of these values, compression axes were constructed (see Appendix A) and plotted. The resulting diagrams were contoured, using the technique described by Kamb (1959). The best preferred orientation of the compression axes was obtained for estimated angles of 45° and 30° (see Figure 9 for one example). In view of this apparent equivalence, an intermediate value of 37.5° was chosen as the most representative angle between slip linear and local axis of compression.

This relatively high angle of failure may indicate that failure in the granite followed pre-existing fractures and mylonitic zones, inclined at angles higher than 30° to the major

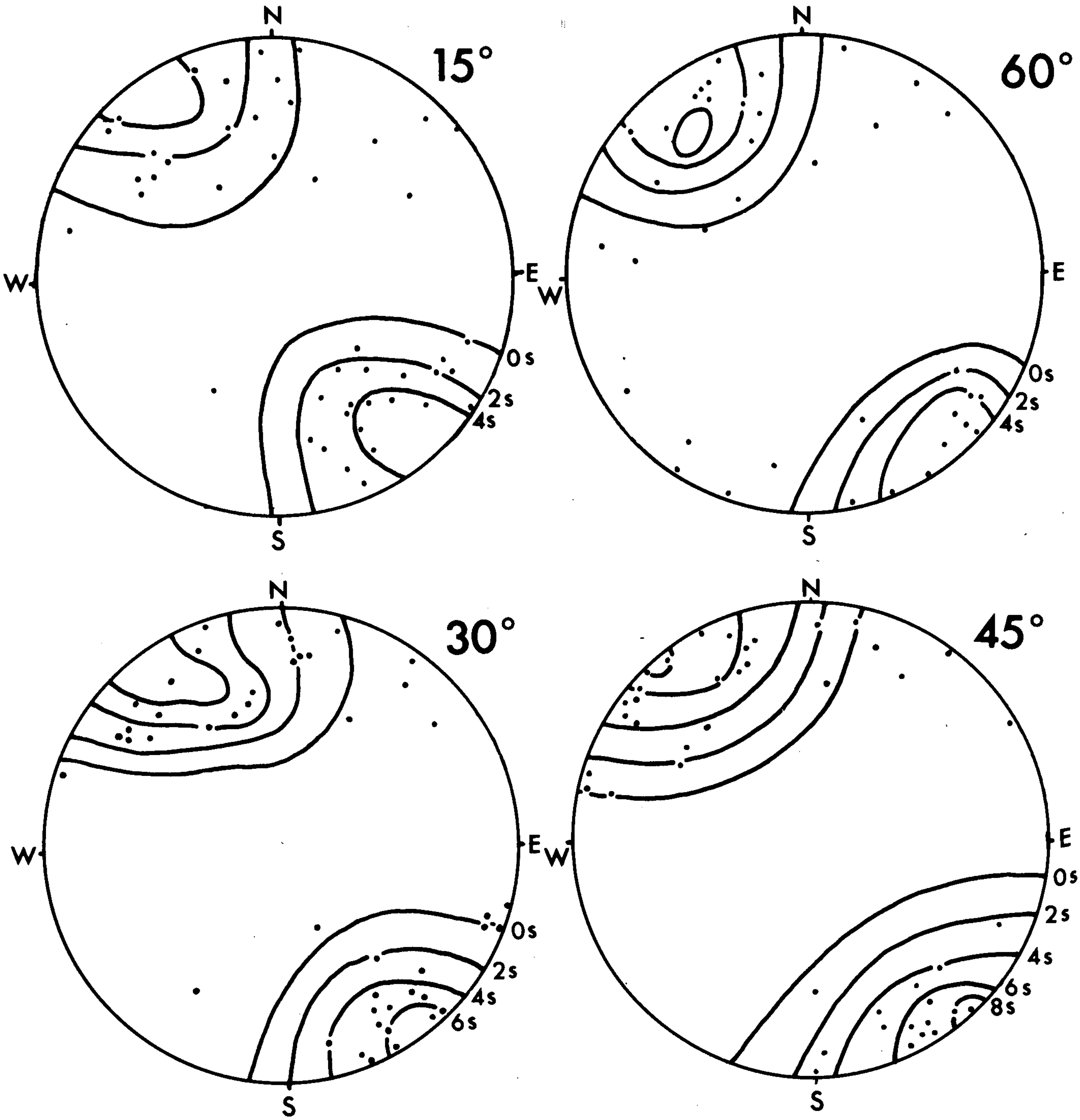

FIGURE 9: Derivation of compression axes from slip linears on fractures in granite with varying angular relationship between compression axes and slip linears. Contour interval 2 standard deviations (Kamb, 1959).

principal compressive stress. σ_2 and σ_3 axes fall along great circles perpendicular to σ_1, but their orientations vary greatly. This observation points to the possibility that during deformation σ_2 and σ_3 had about the same magnitude.

Statistically the major principal stress is oriented subhorizontally in a north-northwesterly direction. In the southernmost part, however, the σ_1 axis is found to be inclined up to 25° to the south.

Axes of compression are shown on the Dynamic Map (marked "G") and Figure 7.

The orientations of local stress fields, derived by the three techniques outlined above, are consistent with each other. They are also compatible with the orientation of bedding-plane slip, flexural-flow folding, thrusting and strike-slip faulting in the area. It is interesting to note that the major principal stress axes have about the same orientation in both basement and sedimentary cover.

5) Quartz Veins, Joints and Regional Stress Relief

Quartz veins are fractures filled with quartz. Two types of quartz veins are found in the region: those formed during the penetrative deformation of the area, and those formed mainly afterwards. Quartz veins, formed during penetrative deformation, generally have gentle dips, rarely exceed a few inches in length, vary greatly in thickness, and are commonly re-deformed, particularly within argillaceous units; those formed after penetrative deformation have steep dips, extend commonly over several feet, are uniformly thin, and cut across earlier deformational structures such as bedding-plane striations and contraction faults.

The two types of quartz veins can be seen to grade into each other; some of the steep thin veins are associated with small offsets in the surrounding bedded rocks (Figure 10).

The steeply dipping, late quartz veins, in turn, grade almost imperceptibly into joints which represent the youngest recognizable fabric element of the area. No offsets were found along or across joints. They occur commonly in groups of closely spaced, very smooth surfaces (Figure 11). Individual smooth joints rarely extend beyond 30 feet; joint groups, on the other hand, may extend over hundreds of feet. Prominent joint groups can be recognized on large-scale air photographs in a very general way.

The joints analysed in the area correspond to systematic (planar) joints of other authors (Nickelsen and Hough, 1967; Hodgson, 1961). They will here be referred to as smooth joints. Non-systematic (non-planar) joints were found to be rare in the Elliot Lake region. Smooth joints can be seen to cut bedding-plane striations, cleavage, contraction faults and flexural-flow folds in many localities. Thus, their late origin

FIGURE 10: Late quartz veins and joints associated with small offset of bedding in Matinenda Formation (Matinenda Lake).

FIGURE 11: Group of smooth joints in Mississagi Formation (Lake of the Mountains).

in the tectonic development of the region is well documented.

The strikes of 830 joints, measuring throughout the area, are plotted in Figure 12a; two trends are seen to predominate: a strong easterly trend and a less pronounced southeasterly trend.

The dip of the joint surfaces is generally steep. It seems to be vaguely controlled by bedding: southerly dipping beds are cut predominantly by northerly dipping joints, northerly dipping beds are cut predominantly by southerly dipping joints. In spite of this general relationship, smooth joints are rarely found to be exactly perpendicular to local bedding, except where bedding is horizontal.

Late quartz veins, individual smooth joints, and groups of smooth joints were measured in the field throughout the area. In addition, prominent joint groups and fracture trends were taken from large-scale air photographs.

Late quartz veins were plotted as great circles on equal-area nets for a number of regional domains. The statistical concentrations of quartz veins in each domain were used to derive generalized diagrams of large quartz-vein orientation. The orientation of quartz veins is shown on the Dynamic Map, and their general trend is plotted on Figure 13.

Individual joints, joint groups and prominent joint groups taken off air photographs are shown with different

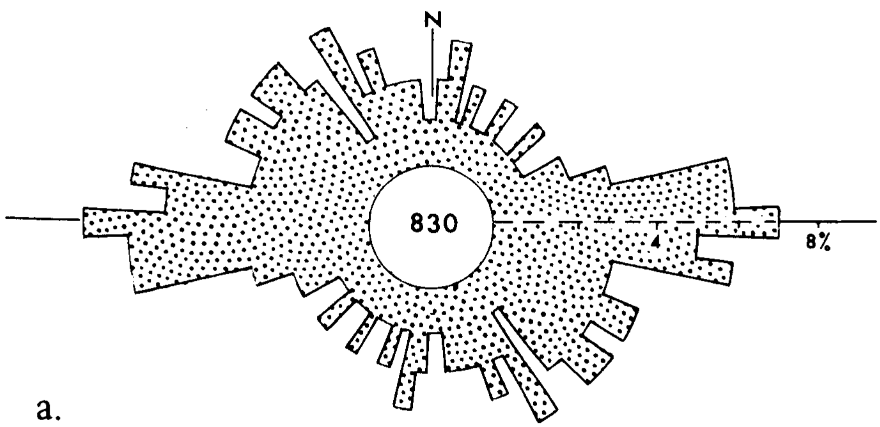

a.

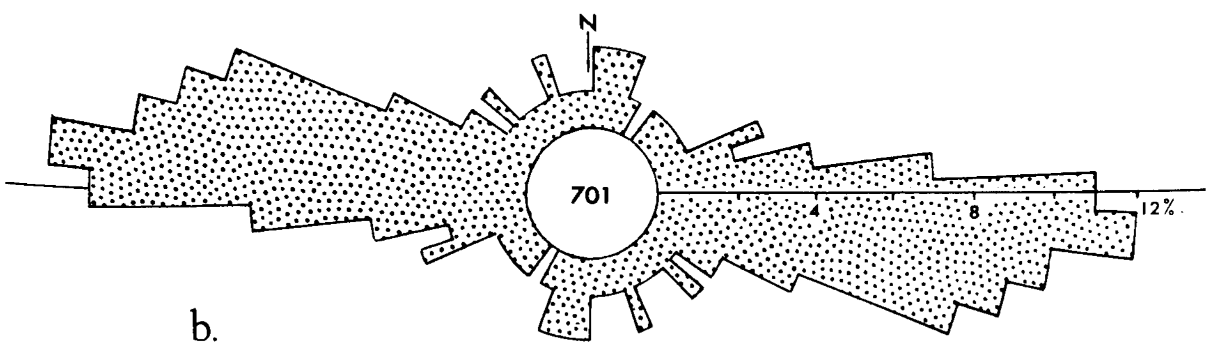

b.

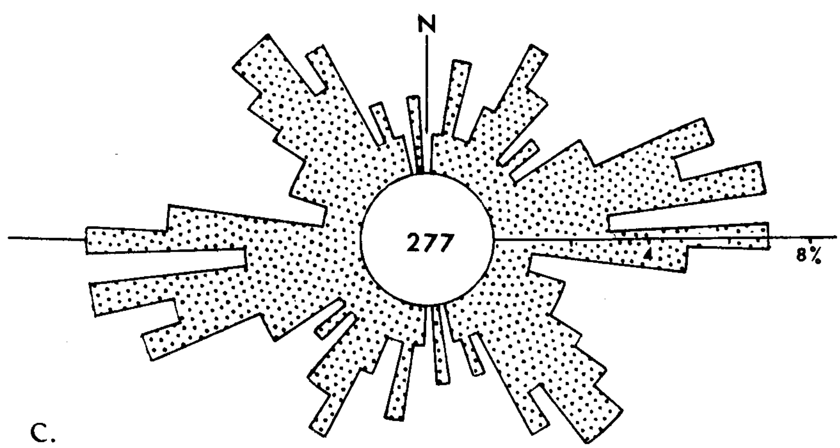

c.

FIGURE 12: Strike frequency diagrams of joints: a) Elliot Lake region, b) Rio Algom Nordic Mine, c) Manitoulin Island. The number of measurements is indicated in each diagram.

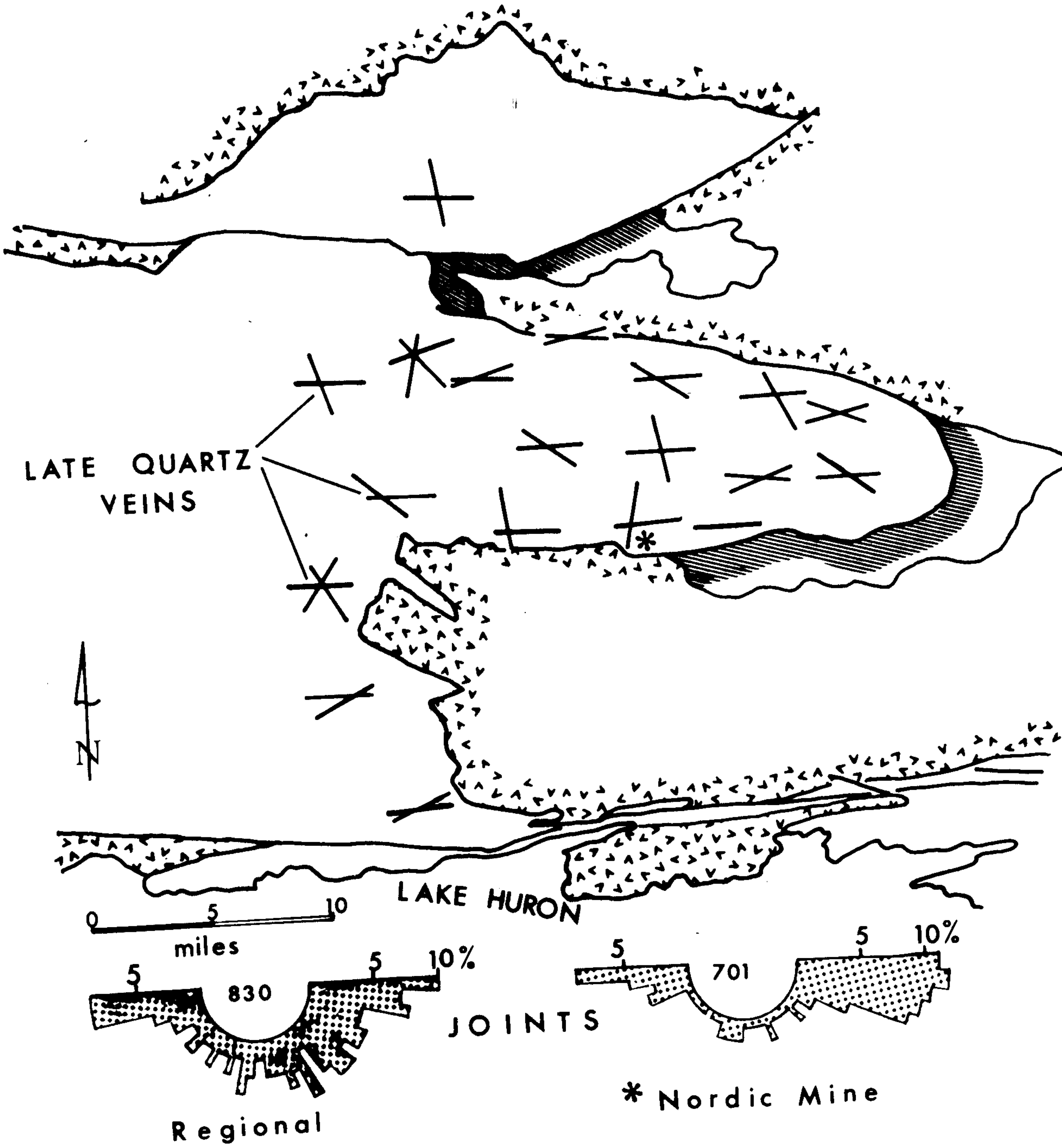

FIGURE 13: Late post-tectonic quartz veins and joint patterns, Elliot Lake region.

symbols on the Dynamic Map.

The significant result from studying late quartz veins and smooth joints seems to be their general equivalence in orientation and mechanism of formation. The late quartz veins and the smooth joints represent local extension. From the Dynamic Map, it can be seen that extension of the rock mass occurred along trends almost perpendicular to the major regional compressive stress, in apparent contradiction to mechanical principles.

It is therefore suggested that differential regional uplifts along easterly trending axes followed the main penetrative deformation of the area, which led to the development of a new stress system. The north-south compressive stresses were greatly reduced and probably dropped below the level of east-west stresses.

It can be speculated that once the first joints formed, stress concentrations built up close to these surfaces immediately after they opened. Growth of successive joints was probably enhanced in these domains. This may help to explain the prominent grouping effect of smooth joints.

Gradual release of tectonic stresses by jointing probably continued throughout the last 1000 m.y. In flat-lying, tectonically undisturbed Lower Paleozoic carbonates exposed on Manitoulin Island, south of the Elliot Lake region (Figure 1), vertical joints show a statistical orientation very similar to that in the Elliot Lake region (Figure 12c). The tectonically undisturbed nature of the carbonate rocks suggests joint propagation from underlying Proterozoic rocks. This process must have taken place later than 400 m.y. ago.

P A R T II

TECTONIC ANALYSIS OF THE RIO ALGOM NORDIC MINE

The orebody at Nordic Mine consists of quartz-pebble conglomerate and interbedded feldspathic sandstone of the lower Matinenda Formation. In the mine area, the Matinenda Formation rests on the greenstone-greywacke complex of the Archean basement. The mine is situated in the southern limb of the Quirke Syncline. The orebody is cut by three large and numerous small easterly trending diabase dykes, which can be found throughout the mine; northwesterly trending diabase dykes are confined to the easternmost part of the orebody. A few diabase sills are also present.

Mining has been carried out in two stratigraphic horizons; east of the major northwest trending dyke, only the upper unit was mined (Figure 14, in pocket). Older workings above and including the sixth level were not accessible. All field observations, therefore, were made below the sixth level of the mine. Although complete rock exposure is available within the mine, it is restricted to a thin stratigraphic interval.

The tectonic fabric of the Nordic Mine fits well into the regional framework established in Part I of this report. It will be discussed under the headings: 1) Kinematic Analysis, 2) Dynamic Interpretation, and 3) Jointing.

1) Kinematic Analysis

Kinematic analysis of the orebody is a synthesis of tectonic fabric elements observed in numerous localities. The orebody was divided into three domains: (A) west, (B) east central, (C) east. The boundary between domains A and B represents an arbitrary choice; domain C is separated from the rest of the orebody by the major, northwest trending dyke (Figure 13). The following tectonic fabric elements, used in the analysis, will be described under the headings: A) Bedding-plane Slip, B) Contraction Faults, C) Steeply Dipping, Striated Fractures, and D) Deformation of Diabase Dykes and Sills.

A) Bedding-plane Slip

Locally, bedding attitudes in the Nordic Mine vary considerably because the bedding surfaces constitute an interlaced network of channel boundaries. Striations along bedding surfaces are rare over most parts of the mine; they are common only in the extreme eastern part, where a stratigraphically higher conglomerate unit has been mined. The direction of bedding slip is generally south-southwesterly (see Figure 14). No significant displacement was observed along the unconformity between Archean greenstones and Matinenda Formation at the numerous localities in Nordic Mine where the contact was investigated.

B) Contraction Faults

Contraction faults cause a local shortening parallel to bedding. Because of the complicated geometry of bedding surfaces within the Matinenda Formation, a planar slip surface may be a contraction fault at one locality and, a few feet away, may constitute slip on bedding.

Most contraction faults dip to the north, slightly more steeply than bedding; striations and offsets indicate south-southwesterly displacements of the hangingwall of a few inches to a few feet. Contraction faults dipping to the south are rare; on these faults, striations indicate a relative displacement of hangingwall to the north-northeast.

In the western part of the mine (domain A), a shatter zone with the characteristics of a contraction fault cuts across the trend of the orebody; it strikes 135° and dips 55° to the northeast (Figure 14). Striations on individual slip surfaces within this zone indicate a relative displacement of the hangingwall to the west-southwest. The slip along the shatter zone is about 10 feet.

C) Steeply Dipping, Striated Fractures

Steeply dipping fractures are common in the Nordic Mine, but only a small percentage are striated. These are planar and continuous; some have been traced for over 500 feet.

The fractures are generally chlorite-coated and widely spaced. They fall into two principal sets with northerly and easterly trends (Figure 14). Striations were found to be subhorizontal; the sense of displacement is shown on a plot of slip linears in Fabric Diagrams A, B, and C (Figure 14). Small changes in orientation, within each fracture set, systematically affect the sense of slip. The maximum displacement on steeply dipping fractures is in the order of a few feet.

Normal and reverse faults described by Bain (1965) coincide with easterly trending, steeply dipping fractures; nevertheless, slip linears indicate subhorizontal rather than vertical displacements along these fractures.

D) Deformation of Diabase Dykes and Sills

Many dykes are cut and offset by bedding-plane slip, contraction faults, and steeply dipping, striated fractures. Internally, dykes are intensively fractured, particularly the smaller ones. Fractures with striations are common; they indicate very complex internal deformation, distinctly different from that of the sedimentary rocks. Calcite filling along the contact between diabase dykes and sedimentary rocks is common; locally calcite-filled fractures are found parallel to the contact within the dykes. Horizontal striations were found on calcite-coated surfaces; the sense of slip along calcite-coated surfaces is the same as that on steeply dipping fractures, with slip linears of the same orientation. The magnitude of slip along the dyke contacts is probably small.

About ten diabase sills were found within the orebody. The sills, generally less fractured than the dykes, are cut by steeply dipping, striated fractures. Striations along the contact between diabase sills and the orebody tend to be oriented in a southerly direction. These slip linears are equivalent to bedding-plane slip, and are plotted as such in Figure 14.

2) Dynamic Interpretation

The conditions for interpreting the orientation of local stress tensors from kinematic data were discussed earlier. In the Nordic Mine, steeply dipping, striated fractures can be used in the dynamic interpretation because their sense of displacement reverses systematically with changes of a few degrees in the orientation of the fracture.

The plane containing the slip linears, in this case the horizontal plane, must also contain σ_1. The direction of σ_1 must be compatible with the sense of displacement observed on the fractures (Figure 14, Fabric Diagrams). The major principal stress (σ_1) for all three domains in the orebody is horizontal and trends north-northeasterly. The orientation of σ_1 is also compatible with slip linears from dykes, bedding planes, and most contraction faults.

Steeply dipping fractures and contraction faults are seen to cut each other; this suggests that slip took place simultaneously on steeply dipping fractures and contraction faults. The orientation of σ_2 and σ_3 is therefore indeterminate in an east-southeasterly trending, vertical plane.

3) Jointing

Planar, smooth joints are common in the Nordic Mine. The orientation of most smooth joints is near vertical, trending in an easterly direction. The rose-diagram in Figure 12b illustrates the frequency distribution of strikes for all joints measured in Nordic Mine. Rose-diagrams for the three domains in the mine are shown in Figure 14. Comparison with Figure 13a shows that the easterly trend of the regional joint diagram is even stronger in Nordic Mine. The southeasterly set of the regional pattern does not occur at Nordic Mine.

The smooth joints within the orebody are surfaces of finite extent - a single smooth joint can rarely be traced for more than 30 feet along strike; in the vertical direction most joints are only partly exposed in mine openings from 9 to 12 feet high.

Smooth joints tend to occur in groups up to 10 feet wide. The spacing within each group may range from a fraction of an inch to one foot. Smooth joints rarely merge; they constitute a stack of individual discontinuities separated by material bridges. Groups of smooth joints are commonly separated by 20 to 30 feet of unjointed rock.

P A R T   III

REASSESSMENT OF ELASTIC-STRAIN-RECOVERY MEASUREMENTS MADE AT NORDIC MINE

In-situ stress fields are generally the result of several sources:

1) Stresses due to natural causes:
   a) Gravitational load.
   b) Current regional tectonic stresses due to subcrustal motions.
   c) Remnant regional tectonic stresses preserved in the rock mass by the interlocking of substances of different mechanical competence. "Residual stresses" in blocks of unconfined rock have been shown to be locked in even on the scale of individual grains (Voight, 1966; Friedman, 1968).
   d) Stresses due to excessive rates of erosion and complex local topography.
2) Stresses due to excavation by man.

<u>Measurements of Elastic Strain Recovery at Nordic Mine</u>

Elastic-strain-recovery measurements obtained by overcoring techniques can be used to determine the magnitude and direction of in-situ stresses in a plane perpendicular to the borehole. Three conditions must be met to calculate stresses from elastic strain recovery: a) the rock is elastically isotropic, b) the stress component parallel to the axis of the borehole is known (Bonnechere and Fairhurst, 1968), and c) the elastic constants of the rock substance are known.

Elastic-strain-recovery measurements at Nordic Mine were reported by Coates (1966); Udd and Grant (1967); Van Heerden and Grant (1967); and Grant (1968). Measurements were carried out in vertical holes (elastic strain recovery in the horizontal plane), and in horizontal holes (elastic strain recovery in vertical planes). Both the USBM Deformation Meter (Coates, 1966) and the CSIR Strain Gauge Strain Cell (Van Heerden and Grant, 1967; Udd and Grant, 1967; and Grant, 1968) were used.

Tectonic analysis (Parts I and II) by the present authors suggests that significant changes in the orientation of the major principal stress took place in the horizontal plane. A reassessment of the measurements in vertical holes was, therefore, considered to be most promising in terms of the tectonic model.

Elastic strain recovery in vertical holes (drilled into the roof) was measured at eight localities (see Figure 14), using the CSIR Strain Gauge Strain Cell technique. Measurements at localities 1 to 7 were reported by Udd and Grant (1967) and Grant (1968); the measurements at locality 8 were made by

H. Bielenstein. Holes 1, 2, 3, 4, 6 and 7 are located along the periphery of the mine; holes 5 and 8 are located in stopes. With the exception of hole 7, which was drilled close to a northwesterly trending dyke, all sites are located in tectonically uncomplicated domains; this could be ascertained as far as drill site examination permitted. Core is only available from hole 8; it contains one bedding-plane slip and two smooth easterly trending joints. Generally, smooth joints constitute the only tectonic fabric element at all sites.

For all sites, field data were converted to magnitude and direction of maximum and minimum strain recovery in the plane of measurement. To plot direction and magnitude of maximum elastic strain recovery for each hole, a graph was developed to present all data as projections on a horizontal plane (see Figure 15). The two coordinate axes of the rectangular reference grid are the geographic east-west and north-south directions respectively. The axes of maximum elastic strain recovery are linked up, starting with the measurement closest to the collar of the drill hole at the origin of the coordinate system. Extension is plotted in the first and fourth quadrants; contraction in the second and third quadrants. In the direction of maximum elastic strain recovery, only extension was found.

The plot (Figure 15) illustrates an apparently

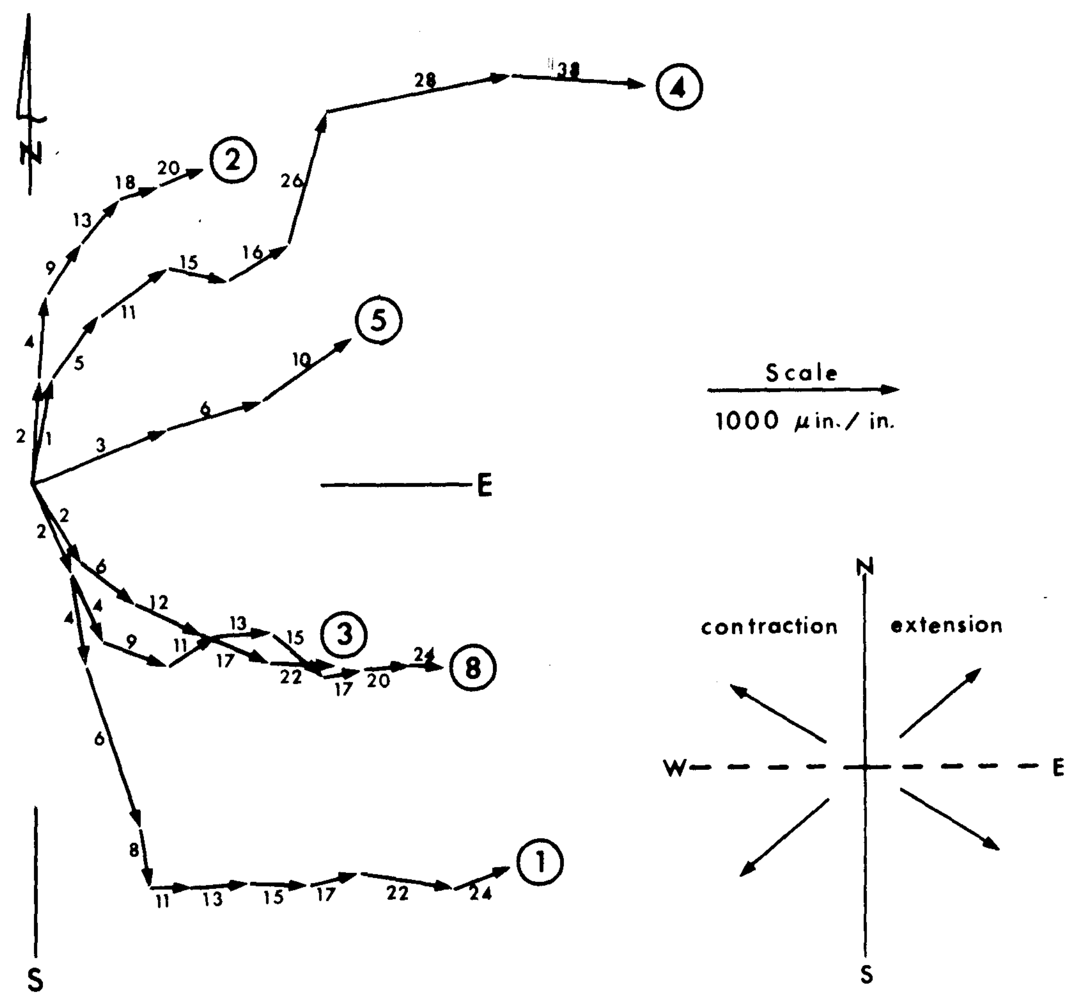

FIGURE 15: Orientation and magnitude of maximum elastic strain recovery in vertical holes ((1) hole number; [15] height of measurement above roof, in feet).

systematic change in the direction of maximum strain components. This change can be abrupt or gradual. The diagram reveals quite clearly that, near the collar, maximum elastic strain recovery tends to line up in a north-northeasterly or south-southeasterly direction; beyond 10 to 15 feet above the collar, it tends to approach an easterly direction. The change in the orientation of maximum elastic strain recovery at about 15 feet above the collar could possibly represent a boundary between two stress environments: a stress environment greatly influenced by mining below the boundary and a field stress environment above.

Holes 6 and 7 were too short to reach this boundary (4.7 and 5.0 feet respectively). Hole 5 seems to be anomalous in respect to the other holes: maximum strain recovery is oriented east-northeasterly throughout the entire length (10 feet). This is the only hole drilled in a north-south trending stope.

The graphical approach used for vertical holes was modified and applied to measurements made in horizontal holes in the abutment zones (Udd and Grant, 1967). Generally, little change in the direction of maximum strain recovery was found. Maximum elastic strain recovery from two holes, drilled near vertical hole 3, are plotted as an example (Figure 16a and 16b). Maximum elastic strain recovery in horizontal holes was found to be generally near horizontal in the abutment zone.

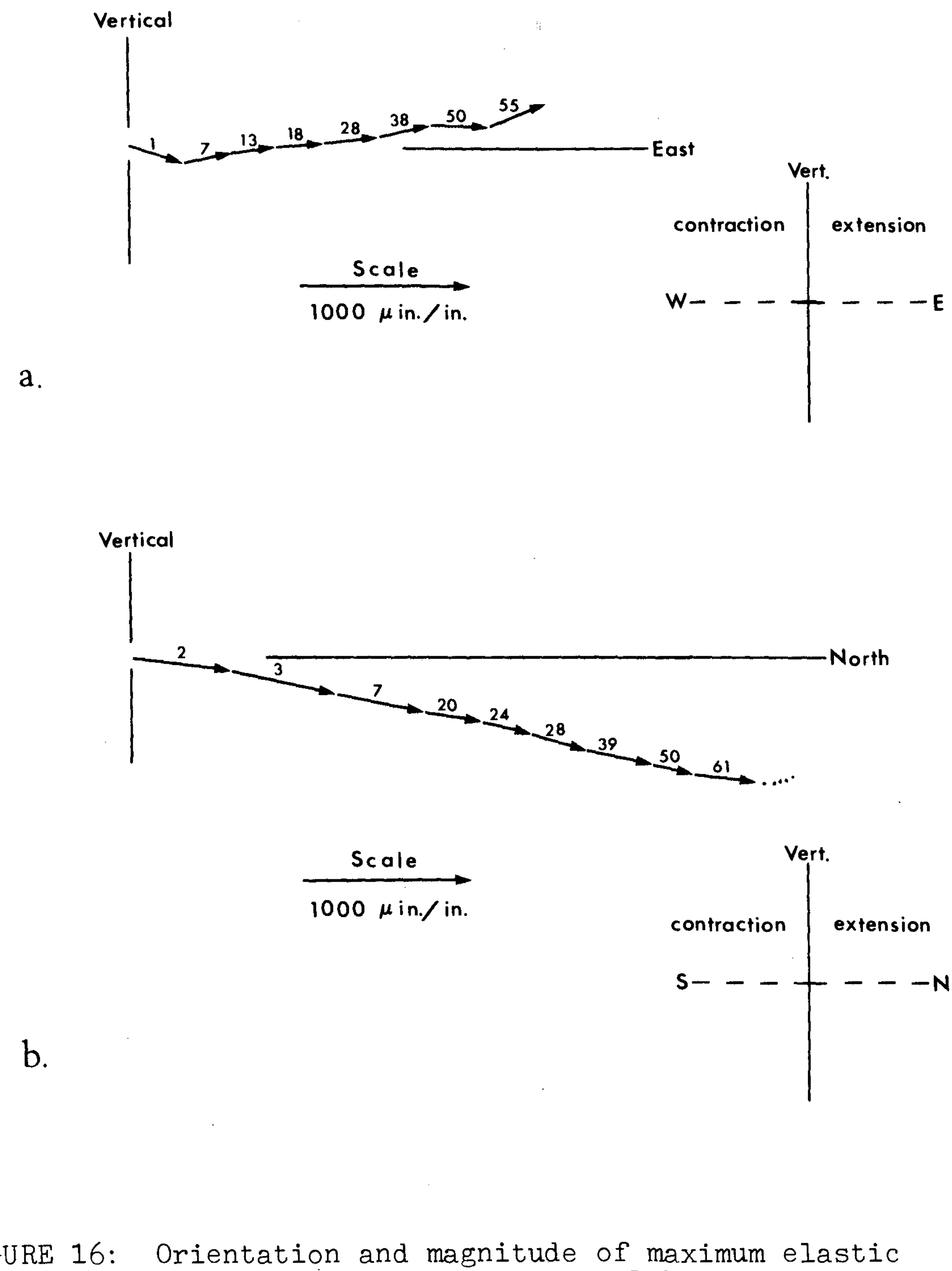

FIGURE 16: Orientation and magnitude of maximum elastic strain recovery in horizontal holes.

a) South, perpendicular to strike of bedding
b) West, parallel to the strike of bedding
(15 distance from collar, of measurement).

Vertical holes seem to offer the unique possibility to separate the influences of two different stress environments.

The magnitude of calculated elastic strain recovery can vary quite erratically. The magnitude of the maximum strain components for all vertical holes and two horizontal holes is plotted against distance from the collar in Figure 17.

Udd (1968 and personal communication) calculated an average field stress for Nordic Mine: σ_1 - horizontal-easterly, 3000 psi; σ_2 - horizontal-northerly, 2500 psi; and σ_3 - vertical, 1500 psi. This average field stress did not include stress determinations within six inches of fractures, visible in core (Udd, personal communication). The maximum stress determined from measurements near fractures tends to be oriented parallel to the maximum stresses determined farther away from fractures (joints), but the magnitude of the maximum field stress is generally higher near fracture (see Udd and Grant, 1967, table 2; Udd, 1968, table 1). This seems to indicate that there is some stress concentration near existing fractures.

Grant (1968) pointed out that there is no obvious relationship between the magnitude of field stresses and local topography or depth below surface at Nordic Mine.

<u>Interpretation of Field Stresses</u>

It is shown in Parts I and II of this report that the local major principal compressive stress axes (σ_1) during

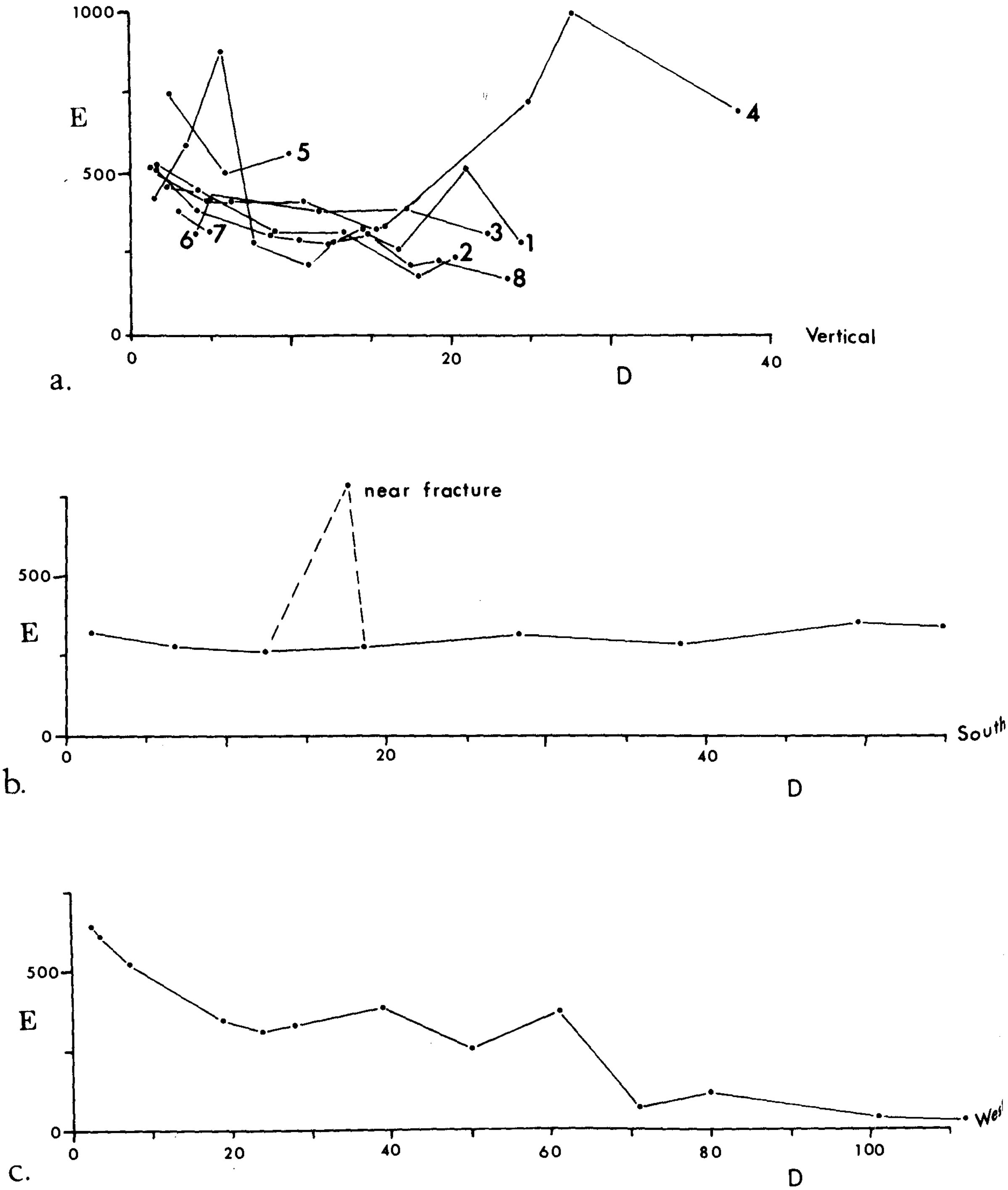

FIGURE 17: Magnitude and location of maximum elastic strain recovery in horizontal and vertical holes.

a) Vertical holes (**3** hole number)
b) Horizontal hole - south
c) Horizontal hole - west
(**E** - strain in μ in./in/;
D - distance from collar in feet).

penetrative deformation were oriented horizontally in northerly directions (Figure 7). The intermediate axes (σ_2) and the minor axes (σ_3) had to lie in an easterly trending plane perpendicular to σ_1. From the observation that contraction faulting and slip along steeply inclined fractures probably occurred simultaneously, it can be concluded that σ_2 and σ_3 were unequal in magnitude locally but that their values were not greatly different on the regional scale.

In order to obtain semiquantitative data on magnitudes of stresses during deformation, two assumptions had to be made:

a) Prior to failure, elastic strains must have built up primarily in the direction of σ_1. One can speculate that principal elastic strains parallel to σ_2 and σ_3 were probably small because of lateral constraints by surrounding rock masses, particularly at great depth. Setting ϵ_2 and ϵ_3 equal to zero, σ_2 and σ_3 are related to σ_1 by the following equation:

$$\sigma_2 = \sigma_3 = \sigma_1/(m - 1) \quad \text{..................(Eq. 1)}$$

m = Poisson's number.

During deformation, overburden in the area probably exceeded 12,000 feet, the minimum value for a composite section of Proterozoic rocks near Elliot Lake (after Roscoe, 1957). For this thickness of overburden, m probably had a value of about 4 (N.J. Price, 1958). Using this value for m, Equation 1 becomes:

$$\sigma_2 = \sigma_3 = \sigma_1/3 \quad \text{.........................(Eq. 2)}$$

b) Furthermore, it has been shown in many triaxial loading tests that the ultimate strength of rocks increases with increasing confining pressure (Handin et al., 1963). Well-indurated quartz sandstone such as the Matinenda Formation, if loaded under simulated overburden of 12,000 feet ($\approx$ 15,000 psi), can sustain differential stresses in the order of 60,000 psi (Handin et al., 1963), assuming very low pore pressure.

From the two hypothetical assumptions, that stresses up to $\sigma_1/3$ were possibly set up along the σ_2 and σ_3 axes, and that ultimate strengths ($\sigma_1 - \sigma_3$ at failure) of 60,000 psi can be maintained under the given overburden, it seems possible that σ_2 and σ_3 **reached values in excess of 20,000 psi. σ_2 and σ_3 would clearly exceed the values to be expected by pure gravitational load.**

Geologic deformation at great depth generally proceeds at very low rates. It seems likely, therefore, that after the ultimate strength of the rocks had been reached, a type of steady-state brittle deformation of the quartzose rock units set in, with stress levels not much below those at which ultimate strength had been reached. Thus considerable amounts of elastic energy remained in the deforming rocks.

It was shown in Part I of this report that late quartz veins and smooth joints postdate the penetrative deformation of the area. It was suggested that there the new stress environment, responsible for the opening of late quartz veins and smooth joints, evolved gradually by unequal stress relief in different directions and not by renewed loading. Jointing indicates that northerly trending stress components suffered the greatest reduction.

The continuity in the evolution of jointing over a long time-span, and the parallelism of maximum elastic strain recovery with the principal joint sets, suggest that the field stresses represent the remnants of former regional tectonic stress fields. It remains to be investigated to what degree residual stress components, locked into the rocks on a grain-to-grain scale, contribute to the field stresses.

In areas with remnant stress fields, late quartz veins and smooth joints may aid in predicting the orientation of field stresses, provided careful tectonic studies are available.

To test this hypothesis, elastic strain recovery must be measured in other parts of the Elliot Lake area to determine if changes in the orientation of late quartz veins and smooth joints are accompanied by equivalent changes in the orientation of the field stresses. In the case of a current tectonic stress field, such a relationship should not be expected, because under conditions of tectonic loading very regular stress fields are the rule (see continuity in the orientation of compression axes in Figure 7).

Highly erratic values in the magnitude of elastic strain recovery, as found in many tests, suggest that differential stresses increase close to jointed domains in the rock mass. To evaluate elastic strain recovery in jointed rock masses, systematic measurements of strain recovery must be made to quantitatively evaluate stress variation around smooth joints. Coates and Grant (1966) suggested the existence of zones of high stresses in Nordic Mine. It remains to be ascertained to what extent such zones are related to particular joint configurations.

ACKNOWLEDGEMENTS

The authors acknowledge the help of the following individuals in this project: Mr. Thos. S. Cochrane, Manager, Elliot Lake Laboratory; Mr. T. Osborne, Deputy Chief Ranger, Ontario Department of Lands and Forests, Elliot Lake; Mr. H.C. Lane and Mr. R.T. Sullivan, Rio Algom Mines Ltd., Nordic Division; Mr. R. Gunning, Denison Mines. Mr. R.B. Park and Mr. A.V. St. Louis ably assisted the authors in the field. Discussions with Dr. D.F. Coates, Mr. J.E. Udd, Dr. D.G.F. Hedley and Mr. G. Zahary helped to clarify the problem. Mr. J.A. Robertson's maps (ODM) were used extensively in the compilation of the Kinematic Map.

The authors are indebted to Dr. M. Friedman (Texas A and M University), Dr. R.A. Price (Queen's University), and Dr. D.K. Norris (Geological Survey of Canada) for critical comments on the manuscript.

REFERENCES

Bain, I. (1965), "The Geological Structure and Probable Rock Stress Environment in the Quirke Syncline and Particularly in the Rio Algom Nordic Mine Test Area, Elliot Lake, Ontario", Mines Branch Divisional Report FMP 65/106, Canada Department of Energy, Mines and Resources, Ottawa.

Barron, K. (1968), "In-Situ Stress Measurements", Internal Report MR 68/119-LD, Mines Branch, Ottawa.

Bonnechere, F. and Fairhurst, C. (1968), "Determination of the Regional Stress Field from 'Door Stopper' Measurements", J. South African Inst. Min. and Met., vol. 68, No. 12, pp 520-544.

Coates, D.F. (1966), "Pillar Loading, Part III: Field Measurements", Research Report R 180, Mines Branch, Ottawa, p 71.

Coates, D.F. and Grant, F. (1966), "Stress Measurements at Elliot Lake", CIMM Bull., vol. 59, pp 603-613.

Collins, W.H. (1925), "North Shore of Lake Huron", Geol. Surv. of Can., Memoir 183, 160 pp.

Compton, R.R. (1966), "Analysis of Pliocene-Pleistocene Deformation and Stresses in Northern Santa Lucia Range, California", Geol. Soc. Am. Bull., vol. 77, pp 1361-1380.

Eisbacher, G.H. (1969), "Regional Structural Study in the Elliot Lake Area, Ontario", Geol. Surv. of Can., Paper 69-1A, pp 158-161.

Eisbacher, G.H. (in preparation), "Contemporaneous Faulting and Clastic Intrusions in the Quirke Lake Group, Elliot Lake, Ontario", Mines Branch, Ottawa.

Fairhurst, C. (1968), "Methods of Determining In-Situ Rock Stresses at Great Depths", Missouri River Division, Army Corps of Engineers, Omaha, Nebraska, Technical Report No. 1-68, 89 pp and Appendices.

Friedman, M. (1963), "Petrofabrics", in Preprints of papers for Intnl. Conf. on the State of Stress in the Earth's Crust, W.R. Judd (ed.), Rand Corp., Memorandum RM 3583, pp 10-1 to 10-124.

Friedman, M. (1968), "X-ray Analysis of Residual Elastic Strain in Quartzose Rocks", Preprint of paper presented at the 10th Symp. on Rock Mech., Austin, Texas, May, 1968.

Grant, F. (1968), "Field Stress Measurements with Encapsulated Rosette Strain Gauge Technique at Rio Algom Nordic Mine, Elliot Lake, Ontario", Internal Report MR 68/49-ID, Mines Branch, Ottawa.

Hast, N. (1958), "The Measurements of Rock Pressure in Mines", Stockholm Sveriges Geologiska Undersokning, Arsbok, Ser. C: 52, No. 3, 183 pp.

Handin, J., Hager, R.V., Jr., Friedman, M. and Feather, J.N. (1963), "Experimental Deformation of Sedimentary Rocks under Confining Pressure: Pore Pressure Tests", Am. Assoc. Petroleum Geologists, Bull. 47, pp 717-755.

Hodgson, R.A. (1961), "Regional Study of Jointing in Comb Ridge - Navajo Mountain Area, Arizona and Utah", Am. Assoc. Petroleum Geologists Bull., vol. 35, pp 1-38.

Hoeppener, R. (1955), "Tektonik im Schiefergebirge: Eine Einführung", Geol. Rdsch., Bd 44, pp 26-58.

Hooker, V.E. and Johnson, C.F. (1967), "In Situ Stresses along the Appalachian Piedmont", Proc. of the 4th Rock Mech. Symp., CIMM and Can. Advisory Comm. on Rock Mech., Ottawa, March 29-30, 1967, pp 137-154.

Kamb, W.B. (1959), Appendix to "Ice Petrofabric Observation from Blue Glacier, Washington, in Relation to Theory and Experiment", J. Geophys. Res., vol. 64, No. 11, pp 1891-1909.

Leeman, E.R. (1964-1965), "The Measurement of Stress in Rock", J. South African Inst. Min. and Met., vol. 65, pp 48-114, pp 254-284, pp 408-423, pp 656-664; vol. 66, pp 109-119.

McIntyre, D.B. and Turner, F.J. (1953), "Petrofabric Analysis of Marbles from Mid-Strathspey and Strathavon", Geol. Mag., vol. 90, No. 4, pp 225-240.

Nickelsen, R.P. and Hough, V.N.D. (1967), "Jointing in the Appalachian Plateau of Pennsylvania", Geol. Soc. Am. Bull., vol. 78, pp 609-630.

Norris, D.K. (1958), "Structural Conditions in Canadian Coal Mines", Geol. Surv. of Can., Bull. 44, 54 pp.

Norris, D.K. and Barron, K. (1969), "Structural Analysis of Features on Nat al and Artificial Faults", Proc., Conf. on Research in Tectonics, (ed.) A.J. Baer and D.K. Norris, Geol. Surv. of Can., Paper 68-52, pp 136-167.

Obert, L. (1962), "In Situ Determination of Stress in Rock", Mining Engineering, vol. 14, No. 8, pp 51-58.

Obert, L. (1966), "Determination of the Stress in Rock--A State-of-the-Art Report", reprinted in Methods of Determining In-Situ Rock Stresses at Great Depths, C. Fairhurst, Missouri River Division, Army Corps of Engineers, Technical Report No. 1-68 (1968).

Pienaar, P.J. (1963), "Stratigraphy, Petrology and Genesis of the Elliot Group, Blind River, Ontario, including the Uraniferous Conglomerate", Geol. Surv. of Can., Bull. 83, 140 pp.

Preston, D.A. (1968), "Photoelastic Measurement of Elastic Strain Recovery in Outcropping Rocks", Trans. Am. Geophys. Union, vol. 49, No. 1, p. 302.

Price, N.J. (1958), "A Study of Rock Properties in Conditions of Triaxial Stress", in Mechanical Properties of Non-Brittle Materials, Proc. Conf. on Non-Metallic Brittle Materials, W.H. Walton (ed.), Butterworth, London, pp 106-122.

Price, R.A. (1967), "The Tectonic Significance of Mesoscopic Subfabrics in the Southern Rocky Mountains of Alberta and British Columbia", Can. J. Earth Sci., vol. 4, No. 1, pp 39-70.

Robertson, J.A. (1961), "Geology of Townships 143 and 144", Ont. Dept. of Mines, Geol. Rept. No. 4, 65 pp.

Robertson, J.A. (1962), "Geology of Townships 137 and 138", Ont. Dept. of Mines, Geol. Rept. No. 10, 94 pp.

Robertson, J.A. (1963), "Townships 155, 156, 161 and 162", Ont. Dept. of Mines, Geol. Rept. No. 13, 88 pp.

Robertson, J.A. (1964), "Geology of Scarfe, Mack, Cobden and Striker Townships", Ont. Dept. of Mines, Geol. Rept. No. 20, 89 pp.

Robertson, J.A. (1968), "Geology of Township 149 and Township 150", Ont. Dept. of Mines, Geol. Rept. 57, 162 pp.

Robertson, J.A., Frarey, M.J. and Card, K.D. (1969), "The Federal-Provincial Committee on Huronian Stratigraphy: Progress Report", Can. J. Earth Sci., vol. 6, No. 2, pp 335-336.

Roscoe, S.M. (1957), "Geology and Uranium Deposits, Quirke Lake-Elliot Lake, Blind River Area, Ontario", Geol. Surv. of Can., Paper 56-7, 21 pp.

Udd, J.E. (1968), "Preliminary Calculations of Stresses in the Abutment Zones, Nordic Mine, Elliot Lake, Ontario", Internal Report MR 68/35-ID, Mines Branch, Ottawa.

Udd, J.E. and Grant, F. (1967), "Measurements of Stresses in the Abutment Zones, Nordic Mine, Rio Algom Mines Ltd., Elliot Lake, Ontario", Divisional Report MR 67/52, Mines Branch, Ottawa.

Van Heerden, W.L. and Grant, F. (1967), "A Comparison of Two Methods for Measuring Stress in Rock", Intnl. J. of Rock Mech. and Min. Sci., vol. 4, pp 376-382.

Van Schmus, W.R. (1965), "The Geochronology of the Blind River-Bruce Mines Area, Ontario", J. of Geology, vol. 73, pp 755-780.

Voight, B. (1966), "Interpretation of In Situ Stress Measurements", Proceedings of 1st Congr. Intnl. Soc. Rock Mech., vol. 3, pp 332-348.

=====

HUB:GHE:(PES)dm

APPENDIX A

SCHMIDT EQUAL-AREA NET

The Schmidt equal-area net is a two-dimensional projection of a reference sphere. It is used to plot the orientation of planar and linear tectonic fabric elements.

Planar and Linear Tectonic Fabric Elements

The orientation of planar tectonic fabric elements can be shown on the Schmidt equal-area net as great circles or points. The great circle represents the intersection of the planar element with the hemisphere; the point represents the intersection of the normal (pole) to the planar element with the hemisphere. A linear tectonic fabric element is shown as a point on the Schmidt equal-area net. The point-density of linear elements or poles to planar elements can be contoured (for techniques, see Friedman, 1963).

Figure 18 shows a planar element (NSD), its pole (P), and a linear element (L) lying in the NSD plane.

Slip Linears

Slip linears are used as a tool to indicate the direction and relative sense of displacement on planar tectonic fabric elements. On the Schmidt equal-area net, the slip linear is a segment of the great circle defined by the striation and

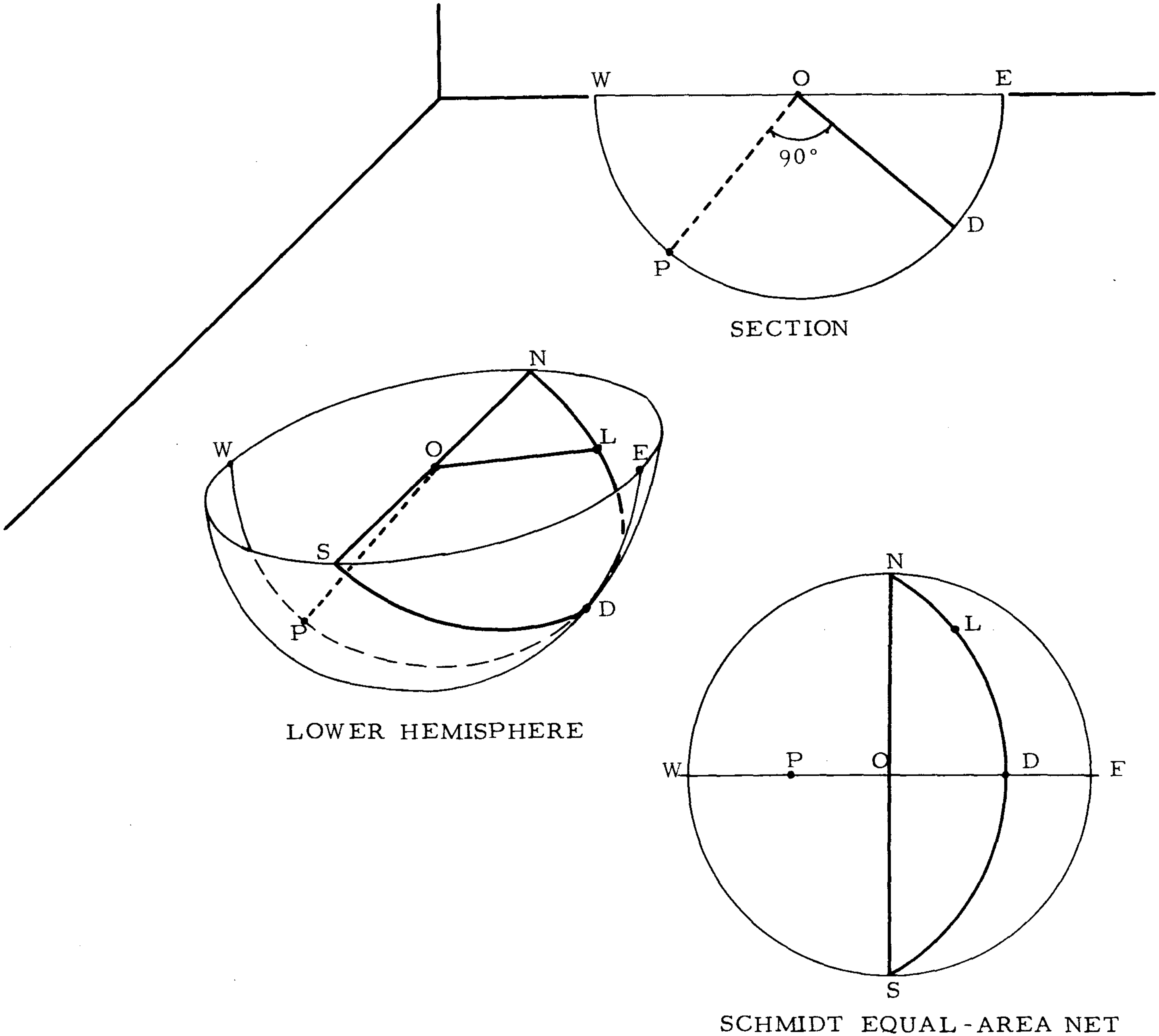

FIGURE 18: Schmidt equal-area projection of planes and lines. See text.

the pole to the planar fabric element containing the striation. Relative displacement of the hangingwall block is indicated by an arrow (Hoeppener, 1955).

Figure 19 shows a striation (OL) oriented east-west parallel to the dip of a planar fabric element (NSD) dipping east. The 'projected slip linear' lies in the vertical east-west plane (WPLE) and passes through the pole (P) to the planar element. The sense of displacement is hangingwall block to the west.

Figure 20 shows a striation (OL) oriented north-south, parallel to the strike of a planar fabric element (NSD) dipping east. The slip linear lies in a west-dipping plane (NSP) and passes through the pole (P) to the planar fabric element. The sense of displacement is hangingwall block to the north.

Compression Axes

If it is found by theory, experiment, or trial-and-error, that certain planar or linear fabric elements can be related to local compression axes (McIntyre and Turner, 1953), construction of compression axes can be carried out on the Schmidt equal-area net. One possible example is shown in Figure 21. It illustrates the construction of a compression axis (OC) which lies in a plane perpendicular to the planar fabric element (WPE) and is inclined 30° to the slip linear (OL).

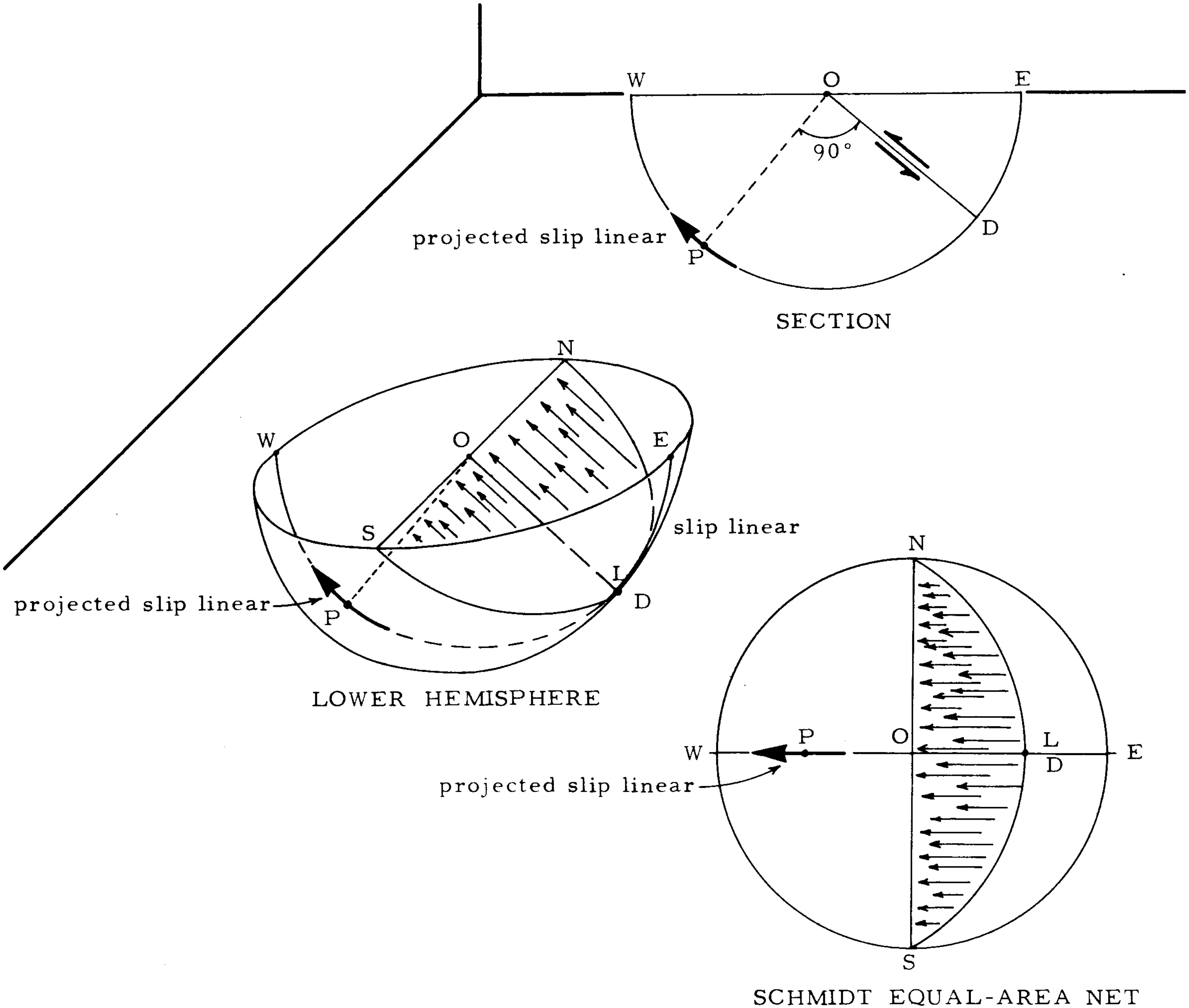

FIGURE 10: Schmidt equal-area projection of striations perpendicular to the strike of a plate. See text.

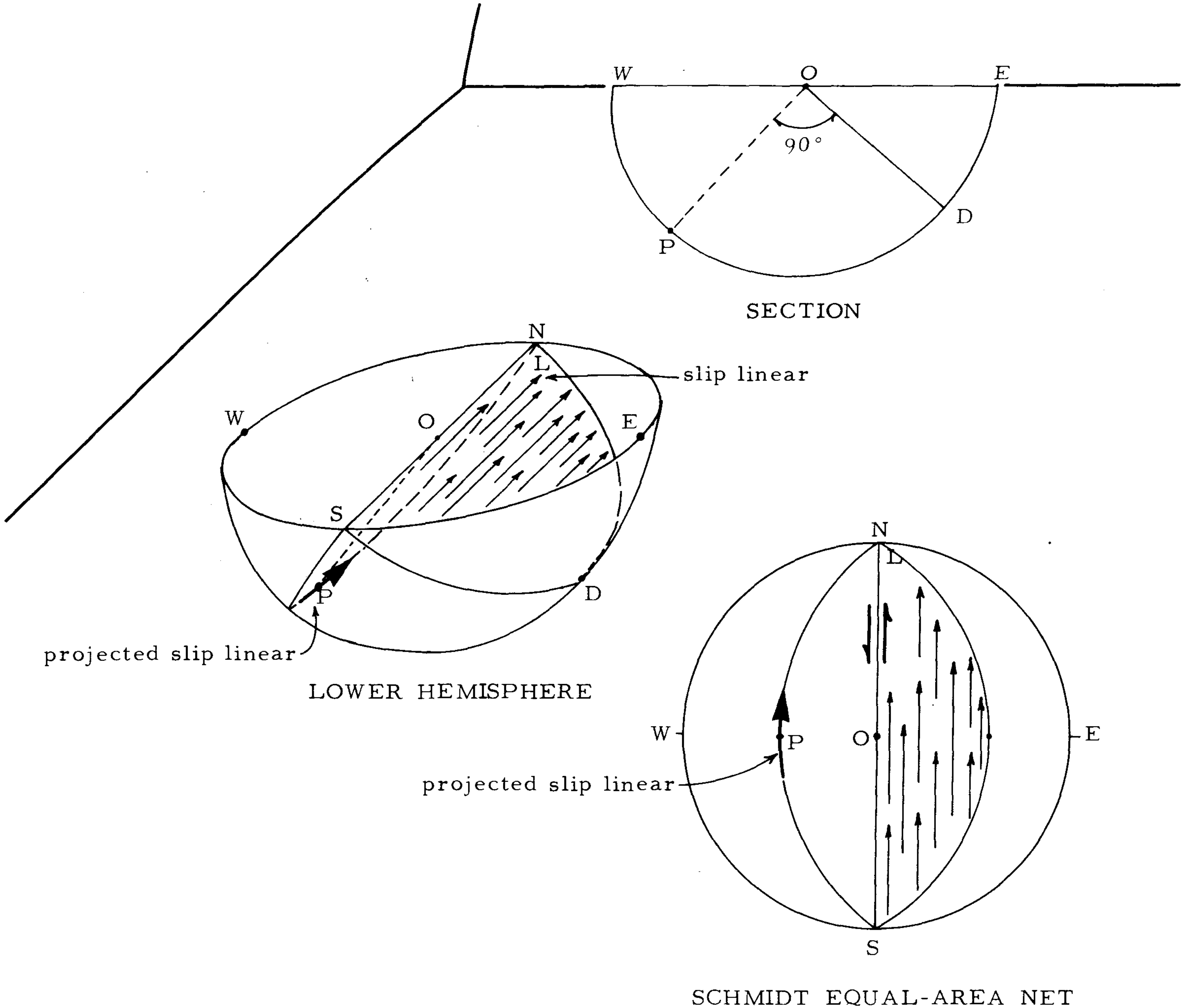

FIGURE 20: Schmidt equal-area projection of striations parallel to the strike of a plane. See text.

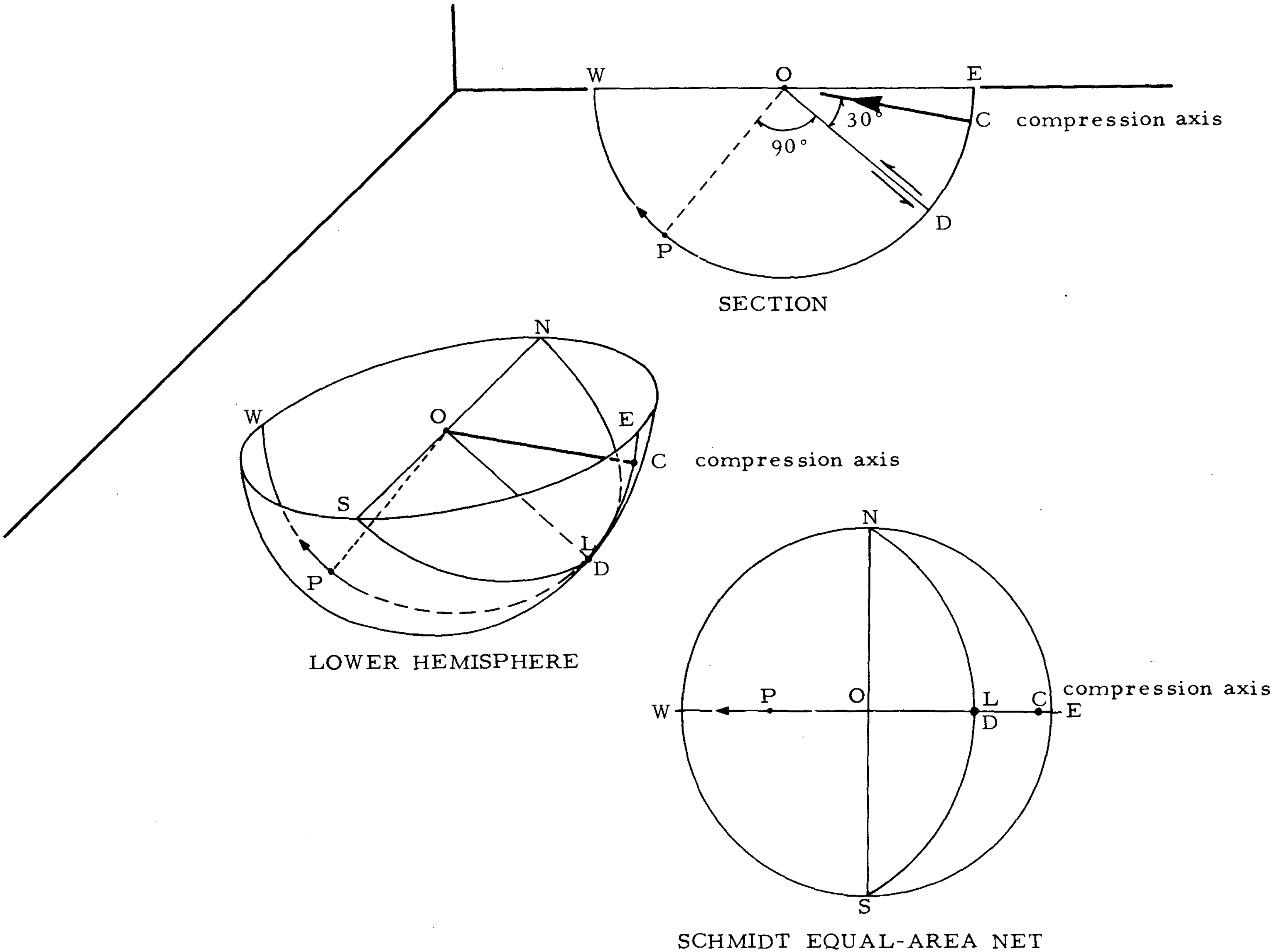

FIGURE 21: Construction of compression axes from slip linears on Schmidt equal-area net.